UNIVERSITÀ
DEGLI STUDI
DI TRIESTE

UNIVERSITÀ DEGLI STUDI DI TRIESTE

XXXVI CICLO DEL DOTTORATO DI RICERCA IN

SCIENZE DELLA RIPRODUZIONE E DELLO SVILUPPO

THREE-DIMENSIONAL EVALUATION OF CAD-CAM GUIDED INSERTION OF PALATAL MINISCREWS

Settore scientifico-disciplinare: MED/28

DOTTORANDA

LUCIA POZZAN

COORDINATORE

PROF. PAOLO GASPARINI

SUPERVISORE DI TESI

PROF. LUCA CONTARDO

ANNO ACCADEMICO 2022/2023

INDEX

LIST OF FIGURES

LIST OF TABLES

ABSTRACT

The confluence of orthodontic mini-screw utilization and the recent digitization integration within the orthodontic field has given rise to protocols, notably the one-visit protocol, designed to optimize resource efficiency, reduce chairside time, and enhance precision and accuracy in fabrication. However, empirical practice has uncovered a frequent incongruity between the anticipated positioning of the palatal miniscrews during the digital design phase and their actual placement after insertion, culminating in the failure of the one-visit protocol and necessitating additional clinical and laboratory procedures. This outcome entails increased waiting time at the doctor's office, increased costs, and delays in treatment commencement.

The primary objective of this study was to evaluate the level of imprecision inherent in each operational phase of the one-visit protocol, with the purpose of identifying its main sources of failure and exploring possible remedies. This investigation involved a three-dimensional examination of the placement of the mini-screw at different stages: during design, the production of orthodontic appliances and clinical mini-screw insertion. Particular emphasis was placed on the distinction between monocortical and bicortical insertions, complemented by Cone Beam Computed Tomography (CBCT) analysis to assess bone quality at the palatal and nasal levels.

The main findings were a similar and laboratory error for the monocortical and bicortical samples (monocortical:1.75° (1.12, 4.79); bicortical: 2.12° ± 1.62, for the bicortical), and a significant deviation between the planned and the achieved position for both samples (monocortical: 4.68° (3.38, 6.51)($p<0.001$); bicortical: 5.70° ± 3.42($p<0.001$)).

Another relevant result was that patients in an earlier maturational stage (MPS1, 2, 3, according to the Middle Phalanx Maturation Method) have a significantly lower palatal cortical bone density (MPS1: 1251.22 ± 2.47.40; MPS2: 1264.28 ± 167.35; MPS3: 1300.21 ± 171.58) than later maturational stages (MPS4: 1485.85 ± 217.70; MPS5: 1638.85 ± 303.25)($p<0.001$), while nasal cortical bone density is more uniform, and generally higher (MPS1: 1424.13 ± 153.32; MPS2: 1379.83 ± 182.96; MPS3: 1488.01 ± 248.48; MPS4: 1489.63 ± 112.18; MPS5 1681.30 ± 323.56).

The findings of these analyses yielded valuable insights that informed the formulation of guidelines for selecting a one-visit protocol over a two-visit alternative, as well as recommendations for optimizing its efficiency and overall success.

1. ORTHODONTIC ANCHORAGE

In orthodontics, tooth movement relies on the transmission of mechanical forces to both bone and the periodontal ligament, initiating a biological response that allows tooth mobility [2]. This process aligns with Newton's Third Law of Motion, wherein an active force generates an equal yet opposite reciprocal force [3]. Orthodontists strategically select anchorage systems to move specific teeth while minimizing reactions in adjacent ones. Anchorage refers to the resistance presented by a tooth to external forces [4] and is crucial in achieving successful orthodontic outcomes.

Orthodontic appliances consist of an active component for tooth movement and a resistance unit providing anchorage. Anchorage can be sourced from neighboring teeth, the palate, the patient's head or neck, or bone implants[5]. There are two primary anchorage categories: intraoral and extraoral [6]. Dental units are the preferred choice for anchorage, supplemented with extraoral headgear if necessary [7]. Simple anchorage, introduced by Angle (1900), uses multiple teeth within the same dental arch as anchors. This method leverages a larger root surface area for increased resistance [8]. The cumulative root surface area of anchoring teeth should ideally be twice that of the teeth to be moved [9]. Connecting teeth with stainless-steel ligatures forms an anchorage block, often useful in molar sites [3]. However, limited evidence exists regarding molar block anchorage capacity [10].

Cortical bone is used to enhance anchorage, necessitating root torquing for contact with the cortical plate. This approach carries risks such as root resorption and loss of vitality [9]. The anchorage potential varies between the maxilla and the mandible, with the alveolar bone providing greater resistance [11]. Transpalatal arches can help maintain arch width and molar position but may not provide sufficient anchorage, particularly in anterior retraction [12] Headgear offers an alternative for extraoral forces, reinforcing anchorage, and enabling various tooth movements [13]. Compliance and risk of injury are factors to consider [7]. Skeletal anchorage, involving endosseous screw insertion, offers greater control and expands the possibilities of orthodontic success. Although ankylosed teeth have been used as anchorage, they are less favored due to surgical complexity, positioning challenges, trauma, and root resorption [14].

1.2 Skeletal anchorage

Miniscrews, also known as Temporary Anchorage Devices (TADs), are widely used in modern orthodontics as skeletal anchorage devices, reducing the need for patient collaboration, and providing optimal results through minimally invasive therapy. TADs offer advantages such as biocompatibility, patient comfort, and secure attachment to orthodontic appliances. Early skeletal anchorage research involved Vitallium screws in dogs [15] and small titanium implants in rabbits [16]. Human cases followed, including teeth intrusion and protraction [17]. Despite advances in dental implants, limitations included size restrictions, invasiveness, and long healing times [18]. To address these limitations, thinner and shorter orthodontic implants were developed. The Orthosystem [19] used a one-piece fixture in the palate, while [20] employed miniscrews between mandibular incisors. Onplant

[21] featured a disk-shaped fixture for maxillary expansion but was invasive. Studies questioned the need for extended osseointegration periods [22].

Titanium orthodontic miniscrews (OMSs) emerged as a key skeletal anchorage method, requiring minimal surgery, and providing immediate mechanical retention due to primary stability. OMS efficiency depends on screw diameter and cortical bone properties. Bone remodeling accelerates with prompt force application, improving anchorage. While partial osseointegration occurs, it doesn't risk failure and allows for screw removal if needed. OMSs, now standard TADs, offer advantages such as smaller size, versatile placement, reduced patient trauma, continuous force application, and shorter treatment durations [4].

2. ORTHODONTIC MINISCREWS

Miniscrews are widely employed in modern orthodontics as skeletal anchorage devices. They significantly reduce the reliance on patient cooperation and ensure optimal outcomes through minimally invasive therapeutic approaches [23]. Miniscrews can serve as support for a conventional anchorage device (indirect anchorage) or as independent anchorage units (direct anchorage). Importantly, they are removed immediately upon completion of orthodontic treatment [24].

2.1 Design and Types

Miniscrews are produced by numerous manufacturers, offering various models, lengths, and diameters, totaling more than 700 different types with 154 designs [25]. Understanding the structural components of TADs is essential for making optimal clinical choices.

Orthodontic miniscrews consist of three main components: the head, core, and the threading (spirals) (Fig. 1). Threading runs throughout the core, leading to two measurable diameters: internal (excluding spirals) and external (including spirals). The core diameter ranges from 1 to 2 mm, but most manufacturers provide external diameter measurements that vary from 1.3 mm to 2.3 mm. Two key parameters for the miniscrew evaluation are the diameter and the pitch of the spiral. The choice of diameter depends on the insertion site and anatomical constraints. Smaller diameters suit narrower sites but decrease fracture resistance. The pitch of the spiral, typically 0.75 mm to 1.25 mm, affects primary stability, with a narrower pitch increasing insertion torque [24].

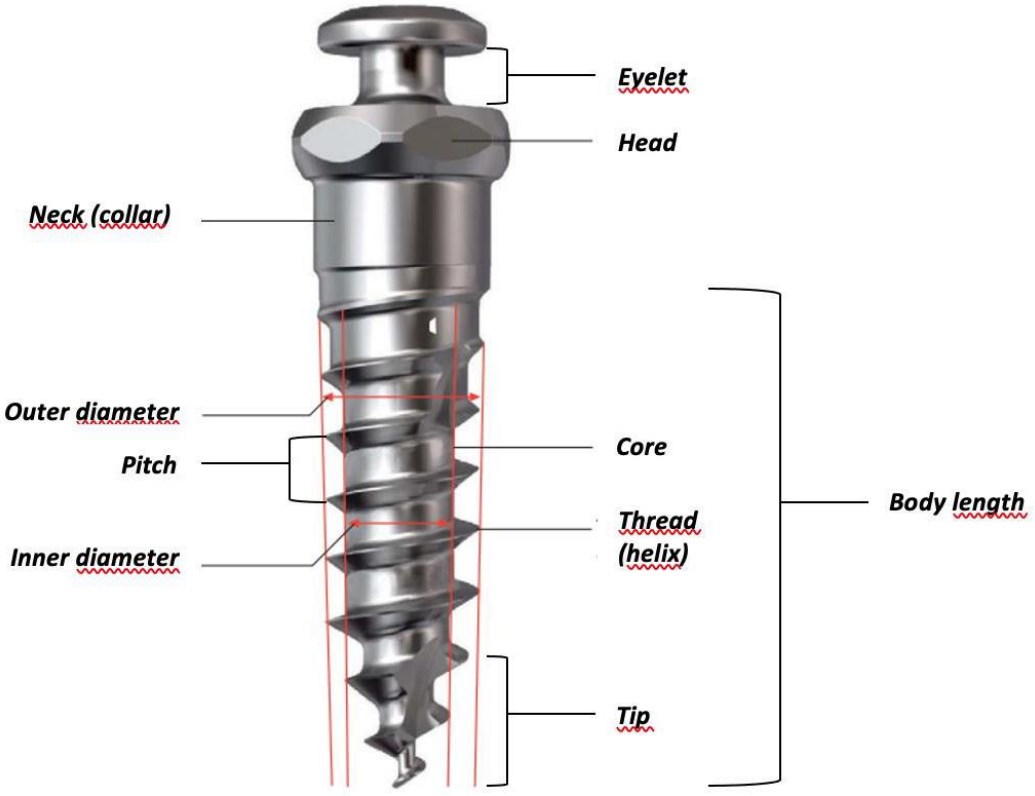

Figure 1: Structure of a miniscrew [24].

Miniscrew heads come in various designs (hexagonal, octagonal, or spherical), which are used based on orthodontic mechanics. The neck or collar connects the head to the core and contacts the transmucosal path. Longer necks find application in areas with thicker keratinized mucosa [24].

Modern miniscrews often incorporate self-drilling tips, eliminating the need for pilot holes. These tips, featuring sharp threading or flutes, perforate bone during insertion. For exceptionally resistant cortical bone, pilot holes may still be advisable. Self-drilling miniscrews reduce insertion time, improve primary stability, and lower post-surgical complications [25].

Miniscrew length, including neck, typically ranges from 6 to 12 mm. The selection depends on the insertion site, such as bone quality, soft tissue thickness, root anatomy, and insertion angle. Longer miniscrews are used for poor-quality bone and can employ the a bicortical engagement for greater primary stability [26]. Miniscrews are commonly made of ASTM grade 5 $\alpha + \beta$ titanium alloy (Ti-6Al-4V), which offers high strength but relatively low ductility [24].

2.2 Insertion and Loading

Precise radiographic evaluation of the insertion sites is crucial to avoid proximity to dental structures and vital anatomical features. Conventional two-dimensional radiographs such as panoramic and periapical may not provide sufficient assessment. Computed tomography (CT) or cone beam CT (CBCT) is recommended for an accurate anatomical study, ensuring improved surgical safety and primary stability during placement [27-29]. Following oral cavity disinfection, local infiltrative anesthesia is administered, and miniscrews are inserted into the cortical bone until fully seated.

The insertion torque represents the force required for the placement of the miniscrew, measured in Newton x centimeter (Ncm). It's influenced by friction during bone perforation and axial thrust for miniscrew advancement [30]. The recommended insertion torque for palatal miniscrews ranges from 10 Ncm to 24 Ncm, impacting primary stability and success rates [31].

Bone thickness and density significantly affect insertion torque. Denser bone requires higher insertion torque for miniscrew placement [32]. Primary stability is correlated with cortical bone quality, while secondary stability is related to medullary bone quality [33-35]. Cortical thickness is a primary determinant of minicrews primary stability. Studies suggest a minimum cortical thickness of 1 mm for good primary stability [36], while a thickness of less than 0.5 mm may compromise miniscrew stability [37].

2.3 Factors Influencing Stability

The success of Temporary Anchorage Devices (TADs) is directly related to their primary stability. Good primary stability, mainly attributed to mechanical retention resulting from the interaction of the miniscrew surface with bone tissue, imparts greater resistance to orthodontic forces on skeletal anchorage devices [38]. Stability is influenced by various factors, including bone properties, particularly density and thickness, the design and type

of the miniscrew, the insertion site, the clinical experience of the operator and the placement technique used [3, 39, 40].

Primary stability arises from the mechanical retention produced by screwing the miniscrew into the bone tissue and is present immediately after appliance insertion, before the onset of the bone healing process. Chen et al. identified primary stability as the most critical factor for the success of orthodontic miniscrews [41].

Secondary stability, responsible for the long-term survival of TADs, results from the biological response of the surrounding bone tissue to the miniscrew. Secondary stability is influenced by the surface characteristics of the mini-screw body, bone tissue characteristics, turnover, and the mechanical retention provided by the miniscrew design [3]. From the insertion of TADs, a bone remodeling process begins, causing primary stability to decrease, while secondary stability increases over time [1] (Fig. 2). The combination of primary and secondary stability constitutes what is known as clinical stability [3].

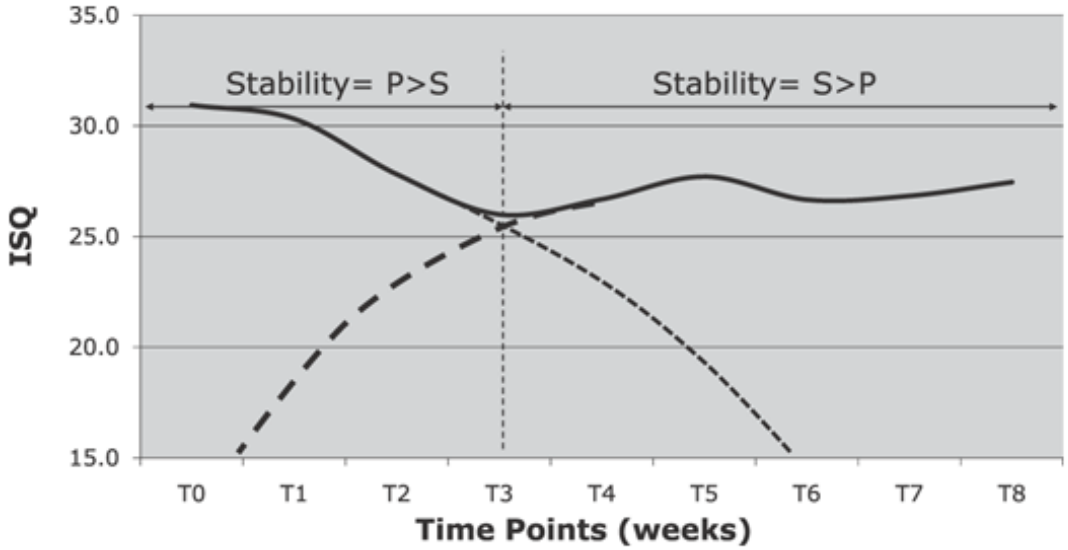

Figure 2: Change in ISQ (Implant Stability Quotient) over time of minivitis that remained stable during an 8-week experimental period, with primary and secondary stability curves (dashed) superimposed 1.

3.PALATAL MINISCREWS

3.1 Palatal Insertion Sites

The choice of the site for the insertion of miniscrews is crucial for primary stability [42]. It is advisable to insert them in adherent keratinized gingival tissue, which is more favorable for their long-term maintenance with a lower risk of inflammation and gingival hypertrophy [42]. The palatal mucosa is composed entirely of adherent keratinized mucosa and, as such, is favorable for the insertion of miniscrews.

Another fundamental factor in the choice of the miniscrew insertion site is the quality and quantity of bone tissue required to ensure good primary stability [25]. At the palatal level, the optimal site considered is in the anterior paramedian area, approximately 4-5 mm from the midline; some authors also suggest the site between the first molar and the second premolar and the palatal vault [37]. The assessment of the insertion site can be performed using second-level radiographic examinations: Cone Beam Computed Tomography (CBCT) is particularly indicated for the possibility of creating surgical guides for miniscrew placement, reducing side effects such as perforation of the nasal cavities, nasopalatine canal, or maxillary sinus [43].

The palate represents one of the ideal sites for the placement of skeletal anchorage devices, ensuring a good position at the point of application of orthodontic forces and a high success rate [44]. Park reported a 100% success rate with the insertion of miniscrews in the anterior palate [44]. These results have also been confirmed by Wilmes et al., who reported high success rates and device stability when inserted in the sites [45].

Ludwig et al. investigated the bone thickness in the anterior palate, using the nasopalatine foramen and the midline suture as radiographic landmarks, to identify the best sites for mini-screw insertion [46] (Fig. 3; Tab. 1).

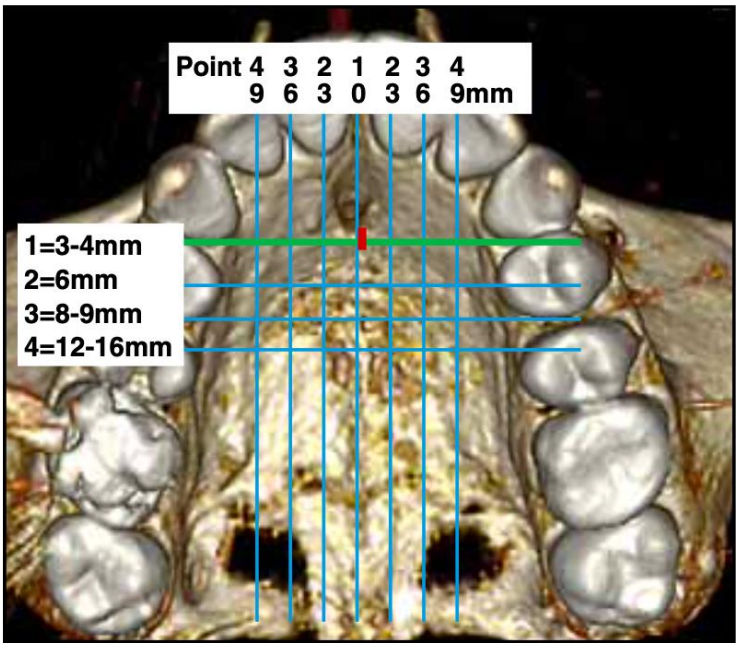

Figure 3: Palatal grid used in the analysis of radiographic and clinical findings (green line: anterior limit within which to insert a palatal miniscrew; red line: distance of the incisor foramen from the reference line) [46]

Table 1: Computed tomography measurements of palatal bone thickness (in mm) at specific grid coordinates (refer to Figure 2 for grid coordinates) [46].

COMPUTED-TOMOGRAPHY MEASUREMENTS (MM) OF PALATAL BONE THICKNESS AT SPECIFIC GRID COORDINATES*

	Lateral Point 1 (suture)		2 (3mm paramedian)		3 (6mm paramedian)		4 (9mm paramedian)	
	Mean	S.D.	Mean	S.D.	Mean	S.D.	Mean	S.D.
Anteroposterior Point								
1 (3-4mm)	7.319	3.057	8.303	0.755	8.060	2.438	5.363	4.201
2 (6mm)	5.785	1.011	6.490	1.004	7.130	0.099	5.855	1.902
3 (9mm)	5.751	0.912	5.317	0.648	5.428	0.807	4.567	0.548
4 (12-16mm)	5.023	0.529	4.004	0.525	3.821	0.543	4.310	1.062

The insertion sites considered most favorable in the literature are the midline and paramedian areas of the palate because a good density and quantity of bone tissue have been found at this location, as well as adequate adherent mucosa [46]. In particular, the optimal insertion site is the anterior region, 3-4 mm posterior to the incisive foramen [46-49]. Furthermore, the risk of iatrogenic damage to vital structures during the insertion of miniscrews in this location is minimal due to lower vascular density and 3-4 mm from the greater palatine foramen [46] (Fig. 4).

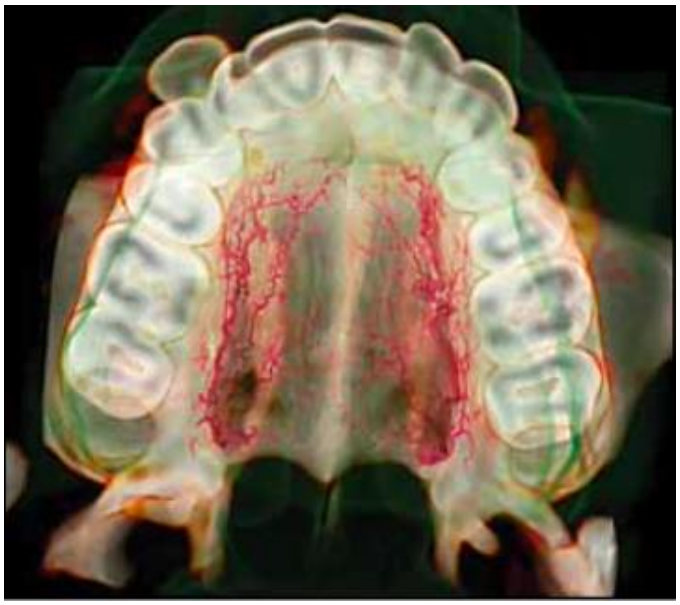

Figure 4:Palatal blood-vessel density [46].

Another palatal insertion site proposed by some authors is in the midline area at the level of the palatal suture. Kim et al. reported a success rate in this area of 88.2% [50]. The choice of this site requires a preoperative evaluation to assess the patient's growth stage because younger patients may have an immature suture, which could be incompatible with miniscrews insertion in this location. Therefore, the literature suggests a thorough preliminary radiographic investigation before planning miniscrews insertion in the midline [51].

Ludwig et al. proposed an additional insertion site at the alveolar level between the first molar and the second premolar. The authors found a favorable inter-radicular space in this location [46], and other studies have shown suitable thicknesses of bone tissue and adherent gingiva for TAD placement [52]. The optimal insertion site in terms of bone quantity is located 8-9 mm apically to the point of contact between the first molar and the second premolar [46].

The main risk factors related to the placement of TADs in the posterior alveolar sectors of the palate, as opposed to the more common paramedian site located 3-4 mm posterior to the nasopalatine foramen, are the abundance of blood vessels and nerve endings at this level and occasional excessive thickness of adherent gingiva [53]. Ludwig et al. defined an area called the "T-zone," considered ideal and safer in terms of relationships with vital structures since it is essentially devoid of major blood vessels and nerves (Fig. 5); this area coincides with the anterior paramedian sites [46].

Figure 5: Potential miniscrew insertion sites in the palate (green=optimal; yellow=restricted areas due to individual variability related to bone thickness; red= unsuitable sites due to thick mucosa or presence of vascular bundles; blue dot= incisal foramen [46].

3.2 Monocortical and Bicortical Insertion

Another factor contributing to the primary stability of the mini screw is the choice of a bicortical anchorage: This involves ensuring that the tip of the miniscrew is anchored to the palatal and lower nasal cortical bone [54]. The choice of the length and insertion axis of the miniscrew, based on accurate preoperative planning considering the thickness of the palatal bone at different sites, allows for a bicortical anchorage. Bicortical anchorage of the miniscrew provides a biomechanical advantage over monocortical anchorage, especially when miniscrews are used as anchorage for orthopedic expansion of the upper jaw in adult subjects, ensuring greater expansion [55, 56]. Therefore, a bicortical anchorage should be considered, especially in complex clinical situations that require stable anchorage against significant loads [54, 57].

3.3 Clinical Applications

Skeletal anchorage in the palate broadens orthodontic and orthopedic treatment possibilities, in some cases eliminating the need for surgery, as demonstrated by Leung et al. in 2008 [58]. Miniscrews allow flexible treatment adjustments, as noted by Ludwig et al. in 2011 [46].

Palatal anchorage appliances come in various forms for treatments such as expansion, mesialization, distalization, intrusion, extrusion, impacted tooth movement, space closure, and tooth uprighting.

Miniscrews revolutionized maxillary expansion, with Miniscrew-Assisted Rapid Palatal Expansion (MARPE) that reduces tooth tipping and timing limitations. Clinicians can choose between hybrid or bone-borne palatal expanders, such as the Hybrid hyrax or the Brolex [59, 60] (Fig. 6).

Figure 6: on the left, a Brölex-type expander; in the middle, traditional expander on 4 miniscrews; on the right, hybrid expander.

For mesial and distal movements, appliances like the Beneslider, Distal Jet, and Pendulum B rely on palatal miniscrews. The MaXimo appliance offers unique anteroposterior action, while others include Fast-Back, Reverse Fast-Back, Keles, Reverse Keles, and Frog Appliance [61] (Fig. 7).

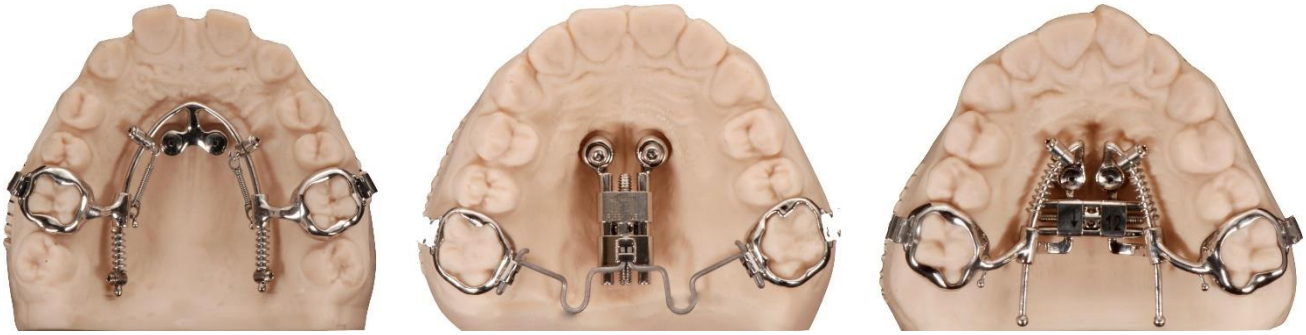

Figure 7: different miniscrew-supported devices to distalize and expand.

For intrusion forces, consider the Mousetrap Appliance, applying effective intrusion forces to molars [62, 63].

4 DIGITAL WORKFLOW IN ORTHODONTICS

In recent years, digital technology has significantly impacted orthodontic procedures, simplified clinical work and aligned with patient expectations. Digital documentation offers advantages such as enhanced orthodontic analysis, rapid diagnoses [64, 65], treatment simulation, improved communication tools, and efficient information sharing among healthcare professionals [66]. It also replaces traditional plaster models with digital ones, saving physical storage space, and enabling Computer-Aided Design/Computer-Aided Manufacturing (CAD/CAM) technology for orthodontic appliance fabrication.

However, adopting a digital workflow involves expenses for equipment and materials [67] and may require training [68]. Digital files can be vulnerable to deletion or loss if not securely stored.

The integration of digital workflows with miniscrews is an evolving area. Clear guidelines have yet to be established, leading to uncertainty among orthodontists about the adoption of digital practices. This section explores various workflows, from palatal miniscrew placement to appliance delivery, and introduces the latest equipment and technologies.

4.1 2-visit Protocol (Traditional and Hybrid Workflow)

Three workflows for palatal miniscrew placement exist: traditional, hybrid and fully digital. In the traditional approach, miniscrews are manually placed within the 'T-Zone' [46] without digital assistance. Orthodontists communicate the miniscrew positions to dental technicians, who use alginate or silicone impressions to create plaster models [69]. Impression abutments are attached to miniscrew heads for reference. The technician assembles the orthodontic appliance, including metal components, fixation rings, and functional arms, using laser welding techniques [61]. After evaluation, the device is delivered to the orthodontist. This method has drawbacks, including challenges in achieving parallelism, potential instability of impressions, and time-intensiveness. In this case, the miniscrews and the orthodontic appliances are placed at two separate appointments, in what is called a *2-visit protocol*.

The hybrid workflow retains the 2-visit protocol and manual miniscrew placement but incorporates digital technology. A scanner is used to acquire a digital model with information about the placement of the miniscrew. A digital STL file is created, converted into a 3D printed model with pre-designed holes for miniscrew analogs, and is then used in the laboratory. STL files are preferred as they are compatible with various design software options [70]. STL files can be obtained through indirect methods, where traditional impressions are scanned, or direct methods, using intraoral scans or CBCT scans. The hybrid workflow reduces the need to store plaster study casts, saves time during treatment, and has been found to produce clinically acceptable digital models in various studies [64-66, 71].

However, it is important to note that results from these studies may vary due to factors like examiner technique errors, material properties, and software programs [72].

4.2 1-visit Protocol (Digital Workflow)

In recent times, digital guidance for the insertion of the palatal miniscrew has emerged [57], with ongoing efforts to improve stability, insertion precision, and reduce complications. A study by Iodice et al. [73] compared manual and 3D-assisted placement of 70 TADs in the anterior palate, finding both methods safe, and favoring digital assistance for less-experienced clinicians.

Digital TAD positioning can expedite orthodontic procedures and accommodate anatomical variations, particularly in complex cases [74]. Although digital workflows lack comprehensive reviews, they rely on implantology software, with certain limitations. Incorporating lateral teleradiography and creating a digital model for dental technicians can still be a challenge. Lateral cephalograms are used for sagittal and vertical analysis, complementing CBCT in cases with limited bone dimensions or anatomical obstacles [75]. Combining lateral teleradiography with intraoral scanning enables a digital workflow for miniscrew placement, simplifying, and speeding up treatment [51].

The workflow involves aligning 2D and 3D images, calibrating the scanner, and selecting landmark points. CBCT scans can be incorporated for increased precision [76]. The most popular software available today can streamline a one-visit protocol, aligning intraoral scans with lateral teleradiography or CBCT scans. Virtual miniscrews are placed, and a surgical guide is designed, using CAD-CAM procedures [57]. Researchers explore fully digital workflows for various orthodontic procedures, such as maxillary expansion [77] and sagittal and vertical dental movements [78], aiming to enhance treatment precision and efficiency. More research is expected to advance the adoption of a fully digital workflow in orthodontics.

5 EXPERIMENTS

5.1 Accuracy of the Digital Workflow for Guided Insertion of Orthodontic Palatal TADs: a step-by-step 3D Analysis

5.1.1 Introduction

The introduction of novel digital technologies within the orthodontic field has made a substantial impact on various aspects of clinical practice and research, from the initial stages of diagnosis to the formulation of treatment plans and the subsequent evaluation of treatment outcomes [79]. A pivotal consequence of this technological progression has been the transformation of guided procedures into digital formats. One of the primary implications stemming from this technological advancement lies in the digitalization of guided procedures for the insertion of palatal Temporary Anchorage Devices (TADs). Through meticulous pre-operative planning and the use of surgical guides, it becomes feasible to achieve precise and controlled TAD placement while concurrently mitigating potential risks associated with this procedure [80, 81].

Numerous studies lend substantial support to the notion that pre-operative planning and the use of surgical guides significantly enhance the accuracy of TAD placement [73, 74, 82]. It is noteworthy, however, that the numerical values regarding deviations in palatal miniscrew positioning between the planned and postoperative positions exhibit considerable variability across studies. This variability arises from disparities in the methodologies used, the software used, and the specific reference points examined. Furthermore, most of these investigations are not clinical, with the majority being cadaveric studies [83] or phantom studies [84]. In a comprehensive overview of the literature, the angular deviations fluctuate between 4.60°±2.54° to 3.67°±2.25° and 3.60°±2.89° [73, 80, 82].

The precision of palatal miniscrew placement becomes particularly pivotal when implementing the one-visit protocol. This protocol, which involves the simultaneous placement of miniscrews and orthodontic appliances in a single appointment, offers a multitude of advantages such as reduced chair time and a streamlined operative process [76, 85, 86]. Numerous case reports document the application of this protocol; however, the need for studies with larger sample sizes is evident to ascertain its efficacy and applicability in routine clinical practice. While these studies do report complications arising from discrepancies between the planned and actual miniscrew positions, they often lack quantification of these complications [69, 76, 78, 87].

Another noteworthy advantage associated with pre-operative planning utilizing Cone-Beam Computed Tomography (CBCT) is the potential for planning a bicortical miniscrew position. Bicortical miniscrews have demonstrated superior stability, improved mechanical outcomes, reduced stress and strain levels, decreased deformation, and fewer instances of fracture [26, 54, 88-90]. Despite the numerous studies highlighting the benefits of bicortical insertion, a frequent omission in investigations relates to whether the inserted TADs were monocortical or bicortical. Notably, there appears to be a dearth of clinical investigations specifically focusing on deviations between the planned and positioned miniscrews when engaging the lower nasal cortical bone.

Given the heterogeneity observed in studies on the accuracy of miniscrew placement and its potential impact on the one-visit protocol, there is a pressing need for a comprehensive assessment of accuracy at each stage of the digital workflow. In particular, to the best of our knowledge, no study has conducted an analysis of the influence of deviations introduced during laboratory processes associated with this specific protocol. The body of literature on medical prototyping elucidates a range of errors, ranging from 0.13 to 0.57 mm, all of which are typically considered within clinically acceptable thresholds [91-94]. Even though the deviations observed in clinical practice have limited clinical significance, it is essential to recognize that potential sources of errors exist at various phases of the prototyping process [91]. Consequently, while most studies conclude that inaccuracies in medical rapid prototyping models are unlikely to have a substantial impact on errors, they have not been able to accurately quantify the individual contributions of each source of error source to model accuracy or determine the minimum acceptable level of accuracy [91-94].

This study seeks to assess the null hypothesis, which posits that there are no significant differences in the angular deviations of Temporary Anchorage Devices (TADs) throughout each stage of the guided digital workflow. The primary objective is to determine which specific operational phase exerts the greatest influence on angular deviations between the planned placement of palatal miniscrews and their actual post-insertion positions. The research approach involves conducting a comprehensive three-dimensional analysis of digital files corresponding to each of the three key stages of the digital workflow, namely, planning, model prototyping, and clinical insertion of miniscrews. Notably, this method offers the advantage of enabling a three-dimensional evaluation without necessitating additional exposure to X-rays. Consequently, this study aims to address the existing literature gap by furnishing an in-depth analysis of angular deviations at each juncture of the digital workflow and providing novel insights into the extent of deviation within a bicortical sample.

5.1.2 Materials and Methods

Patients requiring orthodontic treatment with a palatal appliance supported by miniscrews were chosen from the Section of Orthodontics at the Department of Medicine, Surgery, and Health Sciences, University of Trieste.

The inclusion criteria were the following:

- Requirement for a palatal orthodontic appliance supported by Temporary Anchorage Devices (TADs), involving 2, 3, or 4 TADs, for various applications such as distalization, mesialization necessitating complete anchorage, orthopedic palatal expansion in postpubertal patients, and orthopedic treatment of Class III malocclusions in prepubertal or pubertal patients.
- The need for a guided surgical procedure and a digital workflow, including scenarios such as anterior crowding, impacted teeth, narrow palates, thick mucosa, and cases requiring precise alignment of miniscrews, particularly in cases involving 4 palatal TADs.

There were no specific restrictions about the age or gender of the patients. However, individuals were excluded if they presented systemic diseases affecting bone metabolism, syndromes or craniofacial malformations, pathological conditions in the maxilla, took medications impacting bone metabolism, had compromised immune defenses, bleeding disorders, or exhibited inadequate oral hygiene [95].

Digital Planning (Step 1)

A one-visit protocol was adopted that involves the insertion of miniscrews and the orthodontic appliance within the same appointment. This protocol followed the planning and insertion procedure outlined by the REPLICA System® (Fig. 1). The initial records used included a cone-beam computed tomography (CBCT) scan (My Ray HyperionX9) and a digital impression of the patient's upper arch and palate (CS3600, Carestream Dental). These records were aligned and superimposed using ViewBox software (dHAL Software, Kifissia, Greece). The miniscrews (BENEft®, psm medical solutions) to be used in the clinical procedure were then selected from a virtual library and positioned based on bone availability and the anticipated orthodontic appliance. By established guidelines, the miniscrews were ideally located in the anterior paramedian region, approximately 4–5 mm from the palatal midline, situated between the second and third palatal rugae, while ensuring appropriate parallelism among the screws and maintaining a sufficient distance from the roots of anterior teeth. The posterior palatal region, specifically the premolar and molar areas, was considered as an alternative option [46, 83, 84, 96]. The miniscrews were strategically planned for bicortical insertion, penetrating both the palatal and lower nasal cortical bone. Subsequently, a surgical guide was virtually designed, guiding pillars and analogs were positioned, and the final planning step encompassed the creation of a digital model with holes (referred to as file 1) for the actual analogs, along with the finalization of the surgical guide (Fig. 8).

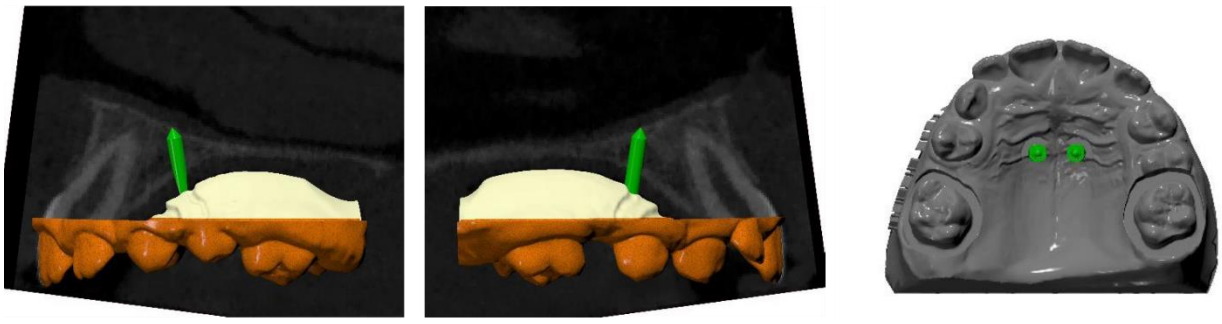

Figure 8: Digital planning of bicortical insertion of two paramedian miniscrews using the REPLICA System®. A, B virtual miniscrews position on the superimposition of cone-beam computed tomography and digital impression. C, coronal view of the position of the virtual miniscrews on the digital model.

Laboratory Procedure (Step 2)

The laboratory phase initiated with the digital design of the orthodontic appliance using Appliance Designer TM software (3Shape A/S, Copenhagen, Denmark). The concluding steps encompassed the prototyping of the model, a digital impression (CS 3600, Carestream Dental) of the prototype with scan bodies (referred to as file 2), the

development of the surgical guide, the sintering of the orthodontic appliance, and the fitting of this device onto the prototype.

Surgical Procedure (Step 3)

Following local infiltrative anesthesia, the surgical guide was positioned to ensure precise alignment and stability. The miniscrews used were BENEft® Orthodontic Screws (PSM Medical Solutions), measuring 2 mm in diameter and 9–11 mm in length. The procedure was carried out using a manually operated unit connected to a contra-angled handpiece (NSK dental). Before miniscrew insertion, a pilot hole was created using a drill equipped with a calibrated drill stop, referencing the CBCT data to ensure penetration solely through the palatal cortical bone. Following the placement of the miniscrew, PEEK scan bodies (BENEft ® system, PSM) were affixed to the screws to capture a digital impression of their actual positions (referred to as file 3). The final step involved the fitting of the orthodontic appliance onto the inserted miniscrews.

Software Analysis

The software analysis was executed utilizing Geomagic Design X (version 2019.0.2). Three files in STL (standard triangle language) format were analyzed for each patient, as follows (Fig. 9):

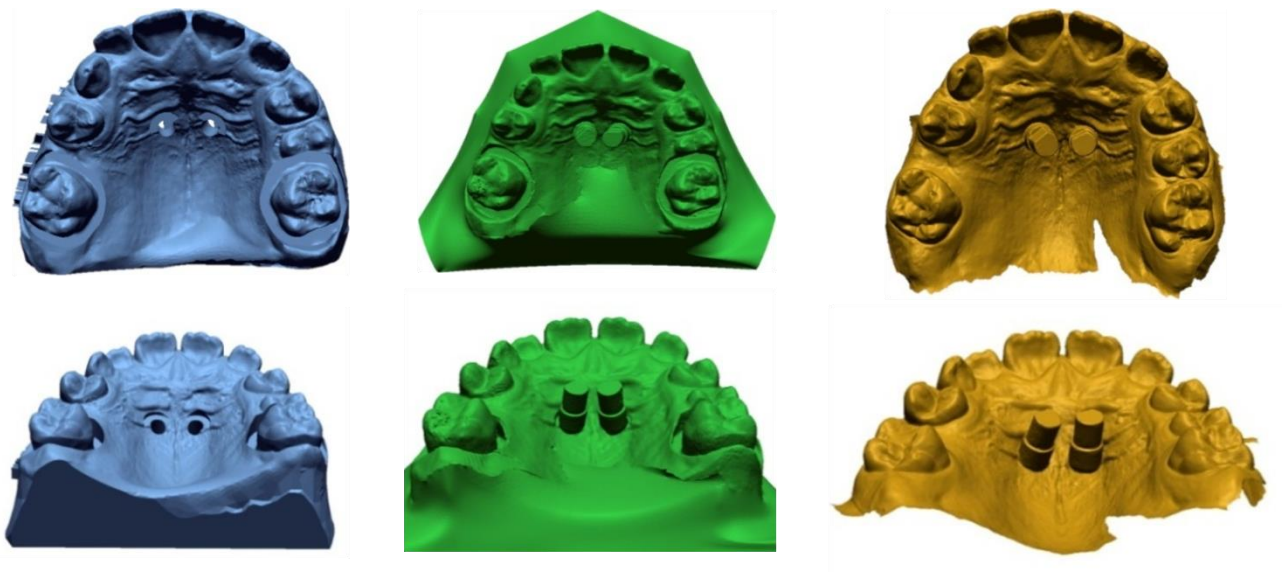

Figure 9: The three fles in STL format were analyzed with Geomagic Design X software (Geomagic Design X- version 2019.0.2). A digital planning of the miniscrews' position (blue); B, scanning of the 3D model with scan bodies for the design and fitting of the orthodontic appliance (green); C, post-insertion digital impression with scan bodies (yellow).

- File 1: The digital plan depicting the virtual position of the miniscrews (a model with holes).
- File 2: A digital impression featuring scan bodies of the 3D prototype, facilitating the fitting of the orthodontic appliance.
- File 3: A digital impression showing the scan bodies that capture the post-insertion positions of the miniscrews after the surgical procedure.

These three files were initially coarsely superimposed using the point-to-point function, with the reference points being the mesiobuccal cusps of the upper first molars and the mesial angles of the incisal edges of the central incisors. Subsequently, a refined superimposition was carried out using an Iterative Closest Point (ICP) algorithm. Once aligned, an automatic shape recognition function categorized each mesh into distinct and well-defined geometric shapes. Each mesh was then individually visualized by selectively disabling the view of the other two. For each of the three meshes, the longitudinal axis of the guiding holes (for file 1) and the scan bodies (for files 2 and 3) was delineated using the "model_add vector_find axis of the cylinder" function, which relied on the automatic identification of cylinders. After establishing the axes, angular measurements were performed to assess the angular deviations between the digital plan and the laboratory model, between the digital plan and the post-insertion position, and between the laboratory model and the post-insertion position, employing the "measure angle_between two vectors" function (Fig. 10).

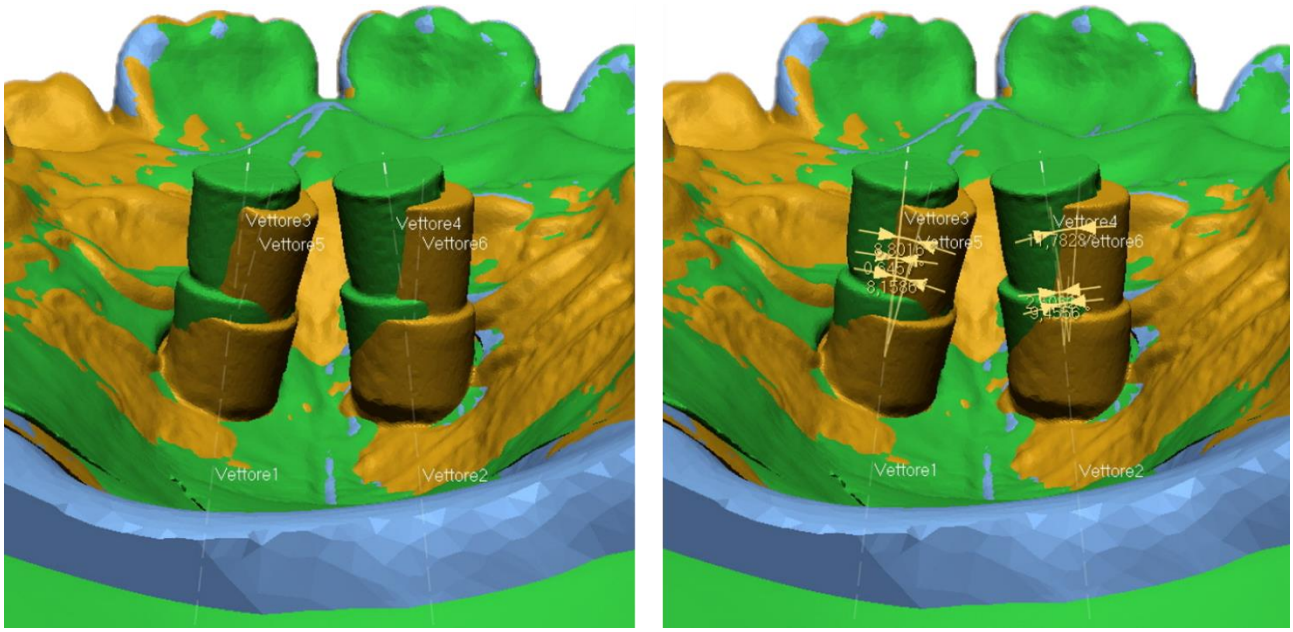

Figure 10: A view of all three files is “switched on” once all the axes are identified; B angular deviations between vectors are calculated.

Error Analysis

A subset of 30 randomly selected measurements was repeated by the same investigator after a two-week interval to assess intra-rater reliability. The calibration was verified using the intraclass correlation coefficient (ICC), which indicated good to excellent interrater reliability (0.93, 0.86–0.97).

Power Analysis

A power analysis determined that a sample size of 45 would provide 80% power to detect a mean of paired differences of 1.5, given a known standard deviation of differences of 3.4 and a significance level (alpha) of 0.05. Data were derived from a previous pilot study (unpublished data). The required sample size was calculated using G*Power (version 3.1.9.7).

Statistical Analysis

Statistical analysis was conducted using SPSS version 26.0 (SPSS Inc., USA), a recognized statistical software package. Descriptive statistics were computed and presented as the median, interquartile range (IQR) and the full range of values. Additionally, mean values along with their respective standard deviations were reported to align with established practices in the existing literature. To validate the assumption of normality, the Shapiro–Wilk test was employed and yielded statistically significant results, signifying a deviation from normal distribution. Consequently, a nonparametric test for related samples was employed to evaluate the null hypothesis, which posits that there are no significant differences in the deviations observed across the three distinct operational stages. Specifically, a Friedman test was executed to compare the deviations across these stages. Furthermore, the Mann–Whitney U test was utilized to assess the significance of differences in deviations between the left and right sides. A predetermined level of significance was established at $p<0.05$ for all statistical analyses.

5.1.3 Results

Participant Demographics and Miniscrew Analysis

A total of 33 patients participated in the study, comprising 18 females and 15 males. The median age of the entire sample was 12 years. Further stratification by gender revealed median age of 13 years for females and 12 years for males. The analysis included a total of 64 miniscrews, with 33 placed on the left side and 31 on the right side. In particular, miniscrews inserted without adhering to the protocol, such as cases involving only partial guidance during surgical procedures, were excluded from consideration. Additionally, cases featuring suboptimal mesh quality that hindered unambiguous analysis were also excluded.

Angular Deviations

Table 2 presents the angular deviations observed in three key aspects: between the longitudinal axis of the miniscrew on the digital plan and the laboratory model (referred to as "Laboratory Deviation"), between the laboratory model and the post-insertion position (termed "Clinical Deviation"), and between the digital plan and the post-insertion position (referred to as "Total Deviation") (Tab. 2).

Table 2: SD Standard Deviation; IQR interquartile range; Lab deviation: the deviation between the digital plan and the laboratory prototype; Clinical deviation: the deviation between the laboratory prototype and the post-insertion position; Total Deviation: the deviation between the digital plan and the post-insertion position.

	Lab Deviation	Clinical Deviation	Total Deviation
Mean	2.12	6.23	5.70
SD	1.62	3.75	3.42
Median	1.65	5.30	5.22
IQR	1.76	3.92	3.96

Range	7.69	16.52	16.70

Operational Step Deviations

Regarding the specific operational steps, the laboratory step, defined as the deviation of the miniscrew's longitudinal axis between the digital plan and the laboratory prototype, exhibited a mean deviation of 2.12° with a standard deviation of 1.62. Conversely, the clinical step, characterized as the deviation between the laboratory prototype and the post-insertion position, displayed a mean deviation of 6.23° with a standard deviation of 3.75. Lastly, the total deviation, encompassing the deviation between the digital plan and the intraoral position, demonstrated a mean deviation of 5.70° with a standard deviation of 3.42.

Statistical analysis of Deviations

To evaluate the potential significant differences among the deviations at each operational step relative to the others, a Friedman test was performed. The results indicated significant differences between the laboratory deviation and the total deviation ($p<0.001$) and between the laboratory deviation and the clinical deviation ($p<0.001$), following Bonferroni adjustments. However, no significant differences observed between the clinical deviation and the total deviation ($p = 0.231$) (Fig. 11).

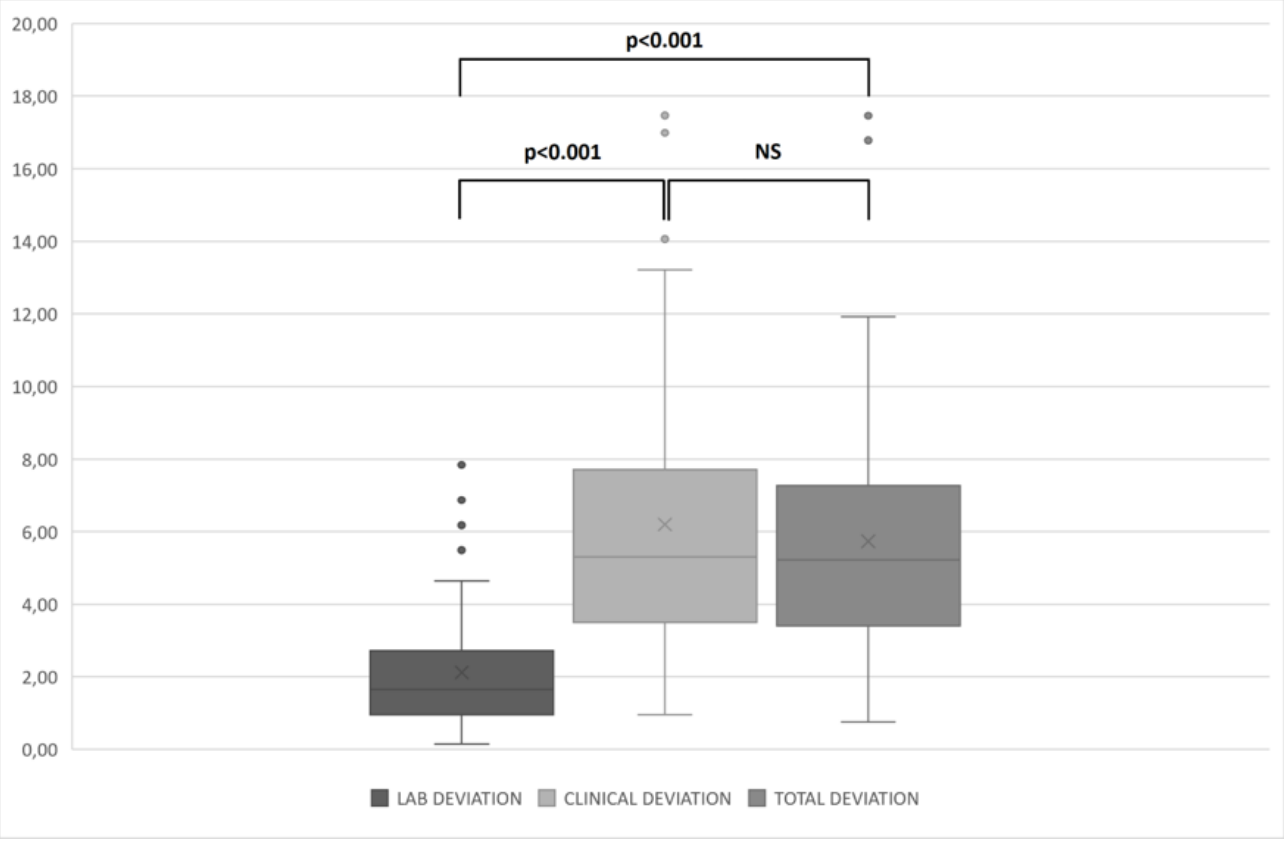

Figure 11: boxplots of the distribution of deviations for the laboratory step, the clinical step, and the total step, and the signifcance of the differences among the steps ($p<0.05$).

Moreover, the study found no significant differences in deviations between miniscrews inserted on the left and right sides.

5.1.4 Discussion and Conclusions

This study aimed to comprehensively investigate the influence of each step within the 1-visit protocol for the guided insertion of palatal miniscrews on the accuracy of the alignment of the miniscrews in their post-insertion position relative to the originally planned position. The null hypothesis that was tested posited that there are no significant differences in the angular deviations exhibited by Temporary Anchorage Devices (TADs) across the three distinct operational stages encompassed by the 1-visit protocol. In our sample analyzed, it became evident that a degree of deviation was introduced at each sequential stage of the workflow. Specifically, the laboratory step, characterized by deviations between the planned digital position and the laboratory prototype (referred to as "laboratory deviations"), displayed an average deviation of 2.12 ° with a standard deviation of 1.62. On the contrary, the clinical step, including deviations between the laboratory prototype and the actual post-insertion position (termed "clinical deviations"), showed a mean deviation of 6.23° with a standard deviation of 3.75. Lastly, the total deviation, which includes deviations between the digital plan and the intraoral position (labeled "total deviations"), demonstrated an average deviation of 5.70 ° with a standard deviation of 3.42.

These findings are consistent with existing literature, suggesting that the medical prototyping procedure is unlikely to introduce substantial errors [84]. However, despite the relatively modest laboratory deviations, their cumulative impact, combined with clinical deviations, has substantial clinical relevance, particularly in the context of a 1-visit protocol. The tolerance threshold for angular deviations decreases as the number of miniscrews, undercuts, and the rigidity of the orthodontic appliance increase. When deviations surpass this critical threshold, it renders the orthodontic appliance ill-fitting, necessitating the adoption of a 2-step protocol [74]. The 2-step procedure involves obtaining a new digital impression of the precise miniscrew positions and modifying the orthodontic appliance, although not without introducing some level of inaccuracy and deviation.

Importantly, the application of the 1-visit protocol, despite its merits in terms of reducing the number of appointments, aims to improve accuracy by limiting the number of operational steps and minimizing transitions between analog and digital workflows [76, 78, 86, 87]. However, our results emphasize that these deviations are not negligible in a clinical context. The angular values observed in this study generally appear to be higher than those reported in the existing literature, although direct comparisons are hindered by variations in reference points and measurement techniques. It should also be noted that no prior studies in the literature have explicitly detailed deviations for a bicortical sample, rendering significant comparisons unfeasible. For monocortical samples, Möhlhenrich et al. report deviations of up to 6.46°±5.5°, a result that closely aligns with the mean value observed in our sample [80].

The increased susceptibility to deviations observed during clinical steps may be attributed to various parameters, both related to the patient and related to the physician. These factors

include bone resistance and density, miniscrew condition, and the clinician's level of expertise of the clinician [83, 97, 98]. In particular, these factors become particularly influential in bicortical cases, where both the palatal and lower nasal cortical bone must be perforated [96]. An intriguing hypothesis that warrants further investigation is that contact with the lower nasal cortical bone during bicortical insertion may introduce an obstruction or a sliding effect, ultimately influencing the insertion path.

It is imperative to consider that the numerical value of deviations is just one aspect requiring attention. Depending on the number of TADs supporting the palatal device, the direction of deviations can be either more favorable, such as when deviations on paramedian TADs compensate for each other, or less favorable, such as when deviations exhibit divergent directions. Moreover, angular deviations can result in linear deviations occurring at the level of the miniscrew head, a situation that has substantial clinical implications for the success of the 1 visit protocol, as well as for the miniscrew tip and all intermediate positions along the insertion path.

This study is subject to certain limitations, which require further investigation of clinical implications. Firstly, while 3D analysis enables a three-dimensional assessment of miniscrew positions without the need for additional x-ray exposure, it remains significantly dependent on the quality of the analyzed meshes. Poorly fitting scan bodies or improper scanning techniques can directly influence the final analysis. However, the existing literature supports the validity and accuracy of scan bodies for assessing implant positions [99]. Additionally, the influence of bicortical insertion on the extent of deviations warrants evaluation through a comparison with a monocortical sample using a comparable workflow.

Concluding Remarks

To the best of our knowledge, this study is the first to comprehensively assess the impact of each step within the digital workflow for guided insertion of palatal miniscrews on the alignment accuracy between planned and final miniscrew positions. Considering the significant influence of clinical steps on angular deviations and the diminishing tolerance threshold associated with deviations, particularly in scenarios involving a higher number of mini-screws or a more rigid structure, the 1-visit protocol is recommended for cases involving only 2 TADs. However, caution is advisable in cases featuring 3 or more miniscrews or a notably rigid structure. In summary:

1. All operational steps contribute to a certain degree of deviation, leading to a cumulative effect.
2. The laboratory step exerts a lesser impact on angular deviations between planned and inserted miniscrews compared to the clinical steps.
3. Cases involving 2 TADs may be successfully managed with a 1-visit protocol, but vigilance is warranted, given the system's reduced tolerance for deviations.

5.2 Does the Planned Miniscrew Position Reflect the Achieved One? A Clinical Study on the Reliability of Guided Miniscrew Insertion Using Lateral Cephalogram and Maxillary Stereolitography File for Planning

5.2.1 Introduction

Miniscrews, known as Temporary Anchorage Devices (TADs), have gained prominence as reinforcement for orthodontic treatments, and their applications have expanded significantly. These versatile devices find utility in both orthodontic and orthopedic contexts. Numerous studies have sought to determine optimal insertion sites and identify key factors to enhance success rates, yielding various success rates across different locations. Specifically, the success rates have been reported as 70.3% for mandibular arch placement, 93.4% for maxillary placement, 98.0% for the anterior palate, and 93.7% for the infrazygomatic zone. In contrast, the buccal shelf exhibited the lowest success and survival rates at 12 months (31.3%) and 24 months (20.8%), with Class III malocclusions demonstrating the lowest survival rate for buccal mini-implants (65.3% and 54.2%) [96, 100-104]. The palatal region is recognized as a reliable and secure site for various miniscrew-supported applications, including distalization, mesialization, and maxillary expansion. Consequently, it is a frequently utilized site in orthodontic practice. Orthodontists planning treatments that involve TADs in the palate can benefit significantly from the use of insertion guides. These guides offer several advantages, including the potential to reduce chair time, often referred to as the "1-visit protocol." They also enable complete control over a digital workflow encompassing miniscrew placement planning, device and guide design, and 3D printing. The guided insertion of miniscrews can be planned using various software tools, which may involve Cone-Beam Computed Tomography (CBCT) or a combination of digital intraoral scans and lateral cephalograms. While the latter approach is limited to median or paramedian insertion sites, both methods culminate in the creation of an insertion guide as the final step. These guides can be fabricated either entirely in 3D printing or through a combination of thermoforming materials and resin. Lateral cephalograms are typically part of the preliminary records maintained by orthodontists. In contrast, CBCT scans are reserved for specific clinical situations or dental issues, such as impacted canines. Consequently, having a dependable digital workflow for miniscrew planning using solely a lateral cephalogram can be advantageous. Furthermore, using an insertion guide, even in a secure area like the anterior palate, could confer clinical benefits by enabling the 1-visit protocol, thereby reducing chair time and the number of appointments. Although several studies have focused on CBCT-based planning [73, 83, 84, 105-107], there is limited scientific literature concerning the precision and reliability of miniscrew placement using a lateral cephalogram, intraoral scan, and thermoformed guide. Therefore, the primary aim of this study is to ascertain whether this approach can ensure accurate miniscrew placement concerning the digital plan and appliance fixation in the context of the 1-visit protocol.

5.2.2 Materials and Methods

Patient Selection and Orthodontic Treatment

This study involved 25 patients (14 females and 11 males), with an average age of 14.2 years, who received consecutive treatment by the same operator (M.M.). The orthodontic treatment comprised the use of a miniscrew-supported device in the anterior palate region, with planned mechanics involving distalization, mesialization, or maxillary expansion. Exclusion criteria included systemic diseases, impacted teeth, the use of drugs affecting bone metabolism, cleft palate, and prior orthodontic treatment. All patients had a permanent dentition.

Data Collection

The initial records for each patient included an intraoral scan (3Shape Trios; 3Shape, Copenhagen, Denmark), photographs, panoramic radiographs and lateral cephalogram X-rays. The orthopal miniscrews used were 1.7 mm in diameter and 8 mm in length (OrthoEasy PAL; Forestadent, Pforzheim, Germany).

Digital Planning and Guide Creation

A single operator imported the maxillary stereolithography (STL) file and lateral cephalogram into dedicated software (OnyxCeph3; Image Instruments, Chemnitz, Germany) and aligned them. The calibration of the lateral cephalograms used the ruler on the acquisition image, while the maxillary STL file was automatically calibrated by the intraoral scanner. This alignment process involved the selection of specific points on the right view of the STL file (buccal side of the central incisors, premolars, and molars) and the lateral cephalograms. The segmented STL file in the sagittal view facilitated accurate alignment with the X-ray (Fig.12).

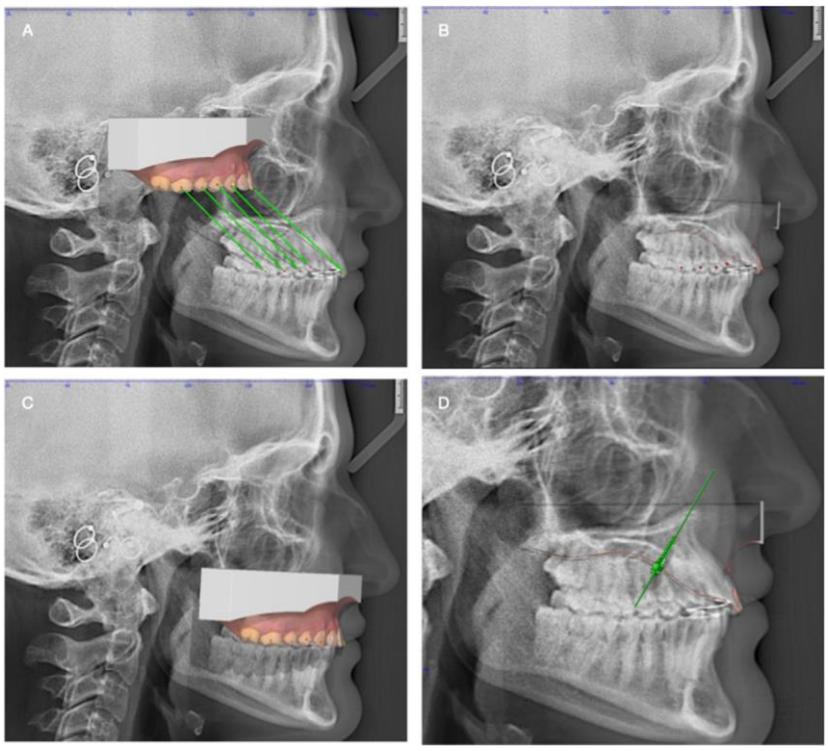

Figure 12: A, STL file and lateral cephalogram references point for alignment. B, The STL maxillary image sagittally segmented for incisor correspondence control in respect of the lateral cephalogram and evaluation of palatal mucosa correspondence to the palatal cortical line. C, STL file and lateral cephalogram superimposed. D, planned miniscrew.

The virtual placement of two miniscrews was performed in the matched file, positioning them in the anterior palate area, using the space between the second and third rugae as a reference. The correct inclination and position were confirmed based on the STL file and lateral X-ray. The lateral cephalograms were used to verify the miniscrew-incisor distance and the maxillary bone depth. The angulation of the buccal-palatal miniscrew was assessed on the STL file using a mean interscrew distance of 9.0 mm. Subsequently, a new maxillary STL file was generated with holes corresponding to the miniscrew positions, followed by the sequential placement of laboratory analogs (Fig. 13).

Figure 13: insertion guide preparation.

The STL file containing the miniscrew positions was 3D printed (DentaModel; Asiga, Alexandria, Australia). The first part of the guide was created by thermoforming 2.5-mm thick polyethylene terephthalate glycol discs (Erkodur freeze; Erkodent, Cologne, Germany). This thermoformed sheet was cropped in the middle to accommodate the screw positions. Miniscrew analogs were then inserted, along with the metal sleeves on the analog heads and the blade used for miniscrew insertion. The final step involved using resin (Leocryl; Leone, Sesto Fiorentino, Italy) to secure the metal sleeves and the thermoformed component.

Surgical Procedure and Post-Insertion Scan

The precision and stability were verified within the patient's mouth. Following local anesthesia, the miniscrews were manually positioned using a surgical key torque (BIOMET 3i, Palm Beach Gardens, Fla). After insertion of the miniscrews, a new intraoral scan was conducted, covering the miniscrew heads with scan bodies to facilitate the post-insertion superimposition process.

Control Group and Data Acquisition

The 3D printed model used to create the guide served as a control group. In all 3D printed models, miniscrew analogs were inserted, and scan bodies were placed over them. A model scan was performed and imported as STL files (control group).

Superimposition and Data Analysis

The planned model (Group P) was uploaded to the TADmatch module (OnyxCeph3, Image Instruments), and miniscrew positions were recorded. Subsequently, the second scan, obtained from the patient's intraoral scan (Group A) or the control scan from the 3D printed model (Group C), was uploaded. The two maxillary scans were registered and superimposed as a surface function. The positions of the "A" miniscrews or "C" analogues were virtually inserted into the first model and exported into an Excel file. The 3D positions of each miniscrew were recorded as XYZ coordinates for the head and tip of the screws. Linear and angular differences were calculated using vectorial formulas between planned miniscrews and achieved (P vs A), between planned and control (P vs C), and between achieved and control (A vs C) (Fig. 14).

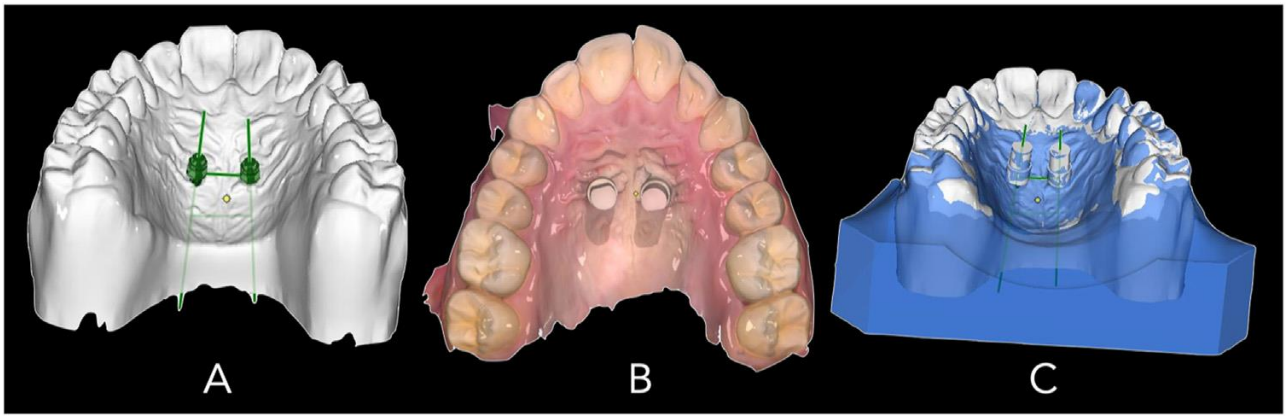

Figure 14: A, STL file with planned miniscrew position. B, Intraoral scan with scan body. C, Superimposition. Second intraoral scans were generally obtained 4-6 weeks after digital planning.

Statistical Analysis

Continuous variables were presented as means with standard deviations and medians with interquartile ranges (IQR), while categorical variables were expressed as the number and/or percentage of subjects. The normal distribution z-test was used to assess the statistical power, with the null hypothesis that the mean of paired differences was 0. The Wilcoxon signed rank test, adjusted using the Bonferroni method, was employed to examine differences in angles determined by the mutual position of two screws among the three different settings. Differences with a p-value below 0.05 were considered statistically significant, and data analysis was performed using R statistical software (version 2018; R Core Team, Vienna, Austria).

5.2.3 Results

Analysis of Achieved and Planned Screw Angles

The median angle observed between two digitally planned screws was 6.22 ° (IQR: 4.35°, 9.08°), and a significant difference was observed compared to the angles in the planning

group (P < 0.001). In the 3D printed model (control) group, the median angle between two parallel planned screws was 1.65° (IQR: 1.17°, 12.76°), and a significant difference was found between these angles and those in the planning group (P < 0.001) (Tab. 3).

Table 3: Angle determined by the mutual position in the space of a couple of screws in a patient with respect to 3 different settings.

Variables	Planning (n=25)	Achieved (n=25)	Model (n=25)	P value	
Angle XYZ	0.00 (0.00, 0.02)	6.22 (4.35; 9.08)	1.65 (1.17, 12.76)	P vs A	<0.001
				P vs M	<0.001
				M vs A	0.315
Angle XY	0.00 (0.00, 0.00)	4.24 (1.51, 7.14)	1.64 (0.84, 12.07)	P vs A	<0.001
				P vs M	<0.001
				M vs A	0.941
Angle YZ	0.00 (0.00, 0.00)	4.43 (2.00, 6.34)	0.96 (0.50, 2.00)	P vs A	<0.001
				P vs M	<0.001
				M vs A	<0.001
Angle XZ	0.00 (0.00, 0.00)	8.59 (3.08, 14.49)	2.36 (1.57, 21.01)	P vs A	<0.001
				P vs M	<0.001
				M vs A	0.482

Note. Values in degrees. Measurements are read in the plane containing both screw directions (Angle XYZ) or between the projections of the directions on the planes generated by the Cartesian axes X, Y, and Z (Angle XY, Angle YZ, Angle XZ, respectively). Results are expressed as median (IQR); P value determined by Wilcoxon signed rank test P value adjusted using Bonferroni method. P, planning; A, achieved; M, model.

Comparison Between the Achieved and Control Groups

No significant differences were observed at the same angle between the achieved result and the 3D printed model (P = 0.315). This finding also held for the projections of the angle on planes generated by the Cartesian axes, except for the projection of the YZ angle on the plane (P < 0.001, Tab. 3).

Angle Deviations of Inserted Miniscrews

Inserted miniscrews exhibited angles of 3.74° (IQR: 2.41°, 6.74°) and 4.68° (IQR: 3.38°, 6.51°) concerning their digitally planned position. In comparison, angles of 4.31° (IQR: 3.15°, 6.58°) and 4.55° (IQR: 3.00°) were observed concerning the 3D printed model (Tab. 4).

Table 4: Angles defined by each screw direction by performing pairwise observations in different settings.

Variables	Angle XYZ (n=25)	Angle XY (n=25)	Angle YZ (n=25)	Angle XZ (n=25)
Planning vs achieved				

Screw 1	3.74 (2.41, 6.74)	2.54 (1.05, 3.68)	2.61 (1.22, 5.12)	3.44 (2.23, 6.25)
Screw 2	4.68 (3.38, 6.51)	2.85 (2.08, 4.09)	3.79 ± 2.54	6.79 (3.61, 8.94)
Planning vs model				
Screw 1	1.61 (0.95, 5.16)	0.83 (0.42, 4.48)	1.12 (0.81, 2.04)	1.61 (0.75, 6.06)
Screw 2	1.75 (1.12, 4.79)	1.69 (0.61, 4.44)	0.89 (0.52, 1.44)	2.10 (1.08, 8.43)
Model vs Achieved				
Screw 1	4.31 (3.15, 6.58)	2.89 (0.63, 6.28)	2.14 (0.72, 3.80)	3.88 (1.18, 11.79)
Screw 2	4.55 ± 3.00	3.11 ± 2.23	2.45 (1.29, 5.08)	5.87 (2.30, 8.27)

Note. Values in degrees. Measurements are read in the plane containing both observed directions (Angle XYZ) or between the projections of the directions on the planes generated by the Cartesian axes X, Y, and Z (Angle XY, Angle YZ, and Angle XZ, respectively). Results are expressed as mean 6 standard deviation or median (IQR).

Linear Displacement of Screws in Each Setting

The linear displacement of the screws in each setting is detailed in Table 5 (Tab. 5).

Table 5: Linear displacement of each screw by performing pairwise observations of it in different settings.

Variables	X (n=25)	Y (n=25)	Z (n=25)
Planning with respect to achieved			
Screw 1 tip	0.20 ± 0.75	0.76 (0.49, 1.21)	1.04 ± 0.76
Screw 1 top	0.08 (-0.07, 0.32)	0.91 (0.75, 1.43)	0.59 (0.29, 0.87)
Screw 2 tip	0.49 ± 0.87	0.87 (0.59, 1.13)	1.16 ± 0.86
Screw 2 top	-0.00 ± 0.51	1.16 ± 0.56	0.55 ± 0.46
Planning with respect to model			
Screw 1 tip	0.02 (-0.19, 0.10)	0.56 (0.20, 0.84)	0.47 (0.25, 0.77)
Screw 1 top	0.11 (0.04, 0.76)	0.54 (0.31, 0.82)	0.43 ± 0.56
Screw 2 tip	0.23 ± 0.42	0.58 (0.37, 0.97)	0.51 (0.37, 0.87)
Screw 2 top	-0.10 (-0.38, -0.04)	0.68 ± 0.52	0.44 ± 0.45
Achieved with respect to model			
Screw 1 tip	-0.30 ± 0.86	-0.45 ± 0.75	0.48 ± 0.68
Screw 1 top	0.01 (-0.17, 0.24)	-0.59 (-0.98, -0.18)	-0.04 ± 0.50
Screw 2 tip	-0.25 ± 0.92	-0.27 ± 0.42	-0.44 ± 0.83
Screw 2 top	-0.19 ± 0.47	-0.49 ± 0.44	-0.10 ± 0.34

Note. Values (in millimeters) are intended in the 3 directions of the reference system (Cartesian axes X, Y, and Z). Positive values indicate that a more lateral (along X), deeper (along Y) or mesial (along Z) displacement has been observed in the cited setting compared to the other one. Results are expressed as mean 6 standard deviation or median (IQR).

5.2.4 Discussion and Conclusions

This study aimed to assess the reliability of a digital workflow for the placement of orthodontic miniscrews in the anterior maxillary area, including the entire process from virtual planning to clinical insertion, following the 1-visit protocol. Streamlining chair time and improving procedure efficiency offer benefits both for clinicians and patients.

The use of digitally planned insertion guides for miniscrews in the anterior area has been proposed in the previous literature as a reliable clinical approach [42, 85, 108]. However, ensuring precision and reliability across all steps of this process is crucial, particularly considering the small dimensions of these screws, which demand minimal vertical and angular errors.

An important aspect of this method is the use of laser-melted structures for orthodontic applications. While computer-aided design and manufacturing processes ensure accurate structure production, some printing imprecisions can occur. Additionally, the rigid nature of the metal alloy used allows for fewer errors and less chairside adaptability.

Previous studies have favored the use of Cone Beam Computed Tomography (CBCT) and stereolithographic insertion guides for miniscrew planning, emphasizing their accuracy over direct methods [83, 84, 108]. However, this study explored virtual planning with a 2D x-ray instead of a 3D image and a thermoformed guide, relying more on technician expertise. This approach is suitable when patients already have lateral cephalograms as initial records and all permanent dentition has erupted [46].

While previous research has compared surgical and direct insertion methods, few have analyzed planned versus achieved positions, a critical aspect for the reliability of the 1-visit protocol. This study identified differences in angular and linear measurements among the three groups. In particular, the largest differences (median, 6.22°) were found between the achieved and planned positions. However, these differences did not cause clinical inconveniences during appliance fixation, suggesting that they were not clinically significant.

Linear discrepancies were observed in all three axes, but they were minimal and did not substantially affect the workflow's performance. Some vertical displacement was noted, with inserted miniscrews not reaching the planned depth (ranging from 0.76 to 1.16 mm). This may be attributed to intraoral scan imprecisions, particularly when compression exists between the scan body base and palatal mucosa during the scan.

The limitations of this study include the use of only a stereolithographic insertion guide. Future research could include a 3D printed guide as another control group and involve multiple operators to validate the procedure from a clinical perspective.

Conclusions

This study draws the following conclusions:

1. The median loss of parallelism between the two screws between planned and achieved positions was 6.22 ° (IQR: 4.35°, 9.08°). Part of this parallelism loss was already observed in the 3D printed model.
2. The median parallelism loss between the 3D-printed model and the achieved result was 4.57°.

5.3 Bone quality in relation to Skeletal Maturation in palatal minscrew insertion sites

5.3.1 Introduction

In contemporary Orthodontics, palatal miniscrews have witnessed a surge in popularity due to their pivotal role in optimizing biomechanics during orthodontic treatments, ensuring absolute anchorage [109-111]. In comparison to alternative insertion sites, the palatal region is deemed safer, primarily attributed to the absence of critical structures like nerves and arteries. Furthermore, the presence of a robust keratinized mucosa renders it a more dependable insertion site than non-keratinized mucosa, collectively contributing to lower failure rates in palatal insertion procedures [35, 46, 112].

Exploring bone density and quantity at palatal insertion sites has been a subject of investigation, primarily through Cone Beam Computed Tomography (CBCT) and Computed Tomography (CT) scans, predominantly in adult patients. These studies have highlighted superior bone quality in locations located 3-6 mm paramedian to the suture and 6-9 mm distal to the incisal foramen [47, 50].

Recognizing that orthodontic treatments are predominantly administered to adolescents; some researchers have delved into bone volume assessments in growing patients. In addition, comparisons have been drawn between CBCT scans of adults and adolescents to discern age-related disparities in bone quality [52, 113]. For example, Farnsworth et al. conducted a study involving 26 adolescents and 26 adults, revealing mean cortical thickness values of 1.25 ± 0.28 mm, 1.07 ± 0.28 mm, and 0.98 ± 0.39 mm dorsal, 6, and 9 mm dorsal, and 3 mm lateral to the incisive foramen, respectively. [37]. This investigation reported an increase in bone thickness in adult patients, speculating that age-related variations in cortical bone thickness could be influenced by hormonal factors and increased muscular activity [114-118]. In a separate study, Han et al. compared 60 adolescents with 60 adults to evaluate differences in cortical and cancellous bone density attributed to age. This examination established that adults exhibited significantly higher bone density (816 ± 15 HU) compared to adolescents (606 ± 14 HU). Likewise, cancellous bone displayed markedly greater density in adults (154 ± 7 HU) relative to adolescents (135 ± 5 HU). [119]. Nonetheless, it is worth noting that previous studies predicated their patient selection on chronological age, a factor that has been previously challenged as an unreliable growth marker. A more reliable alternative to assess skeletal age is the Middle Phalanx Maturation Method (MPM) of the third finger [120-122]. This system has garnered favor among orthodontists owing to its minimal radiation exposure, ease of execution, and interpretability, facilitating close monitoring of ossification events. The MPM method serves as a consistent growth indicator, exhibiting commendable diagnostic accuracy in pinpointing the mandibular growth peak [123, 124].

Consequently, this study seeks to explore the nexus between bone quality at palatal insertion sites and skeletal maturation, as evaluated using the MPM method in growing patients. The overarching objective is to shed light on the potential impact of bone quality on the stability of palatal miniscrews in growing patients, offering information on potential clinical implications and indications for bicortical insertion. The null hypothesis posits that

there exists no discernible relationship between bone quality, characterized by density and thickness, and stages of skeletal maturation.

5.3.2 Materials and methods

Database Selection and Inclusion Criteria

The Orthodontics Section of the Department of Medical, Surgical, and Health Sciences at the University of Trieste, Italy, conducted a database screening that included records compiled between January 2015 and December 2021. The study sample comprised individuals seeking orthodontic treatment, all of whom provided signed informed consent. Ethical approval for the protocol was granted by the University of Trieste's Ethical Committee (protocol code n. 122, date of approval May 23rd, 2022).

The inclusion criteria for this investigation were as follows:

1. Age falling within the range of 8 to 16 years.
2. Absence of anomalies in the maxillary region.
3. Good general health.
4. No history of trauma in the maxillary region.

On the contrary, the exclusion criteria were as follows:

1. Radiographs characterized by substandard diagnostic quality.
2. Individuals presenting with known craniofacial or other conditions or syndromes.
3. Scans indicating palatal impacted permanent teeth in the measured quadrant.
4. A history of prior orthodontic treatment.

For each participant, a radiograph of the middle phalanx of the third finger was taken as a routine clinical record, and a Cone Beam Computed Tomography (CBCT) scan (Hyperion X9, My-Ray, Cefla sc. 40026 Imola (Bo) Italy, www.my-ray.com) was performed as a secondary diagnostic investigation to assess impacted teeth positioning or palatal miniscrew insertion sites. The right quadrant of the maxilla was selected for analysis, and the left quadrant was examined if the scans showed unerupted teeth on the right side, in accordance with the literature that indicated that there were no significant differences in cortical thickness and bone density between the two sides [47, 125-127].

A total of 60 patients were chosen, with a median age of 12 years. This group comprised 11 patients at MPS1 stage (median age 10 years), 14 at MPS2 (median age 12 years), 12 at MPS3 (median age 13 years), 10 at MPS4 (median age 13 years), and 13 at MPS5 (median age 14 years).

Data Analysis and Measurements

CBCT scans were imported into a medical image viewer (Horos Open-Source Medical Image Viewer, version 3.3.6, www.horosproject.org) for the analysis of DICOM files. Prior to measurements, each site was oriented in all three spatial planes (Fig. 15).

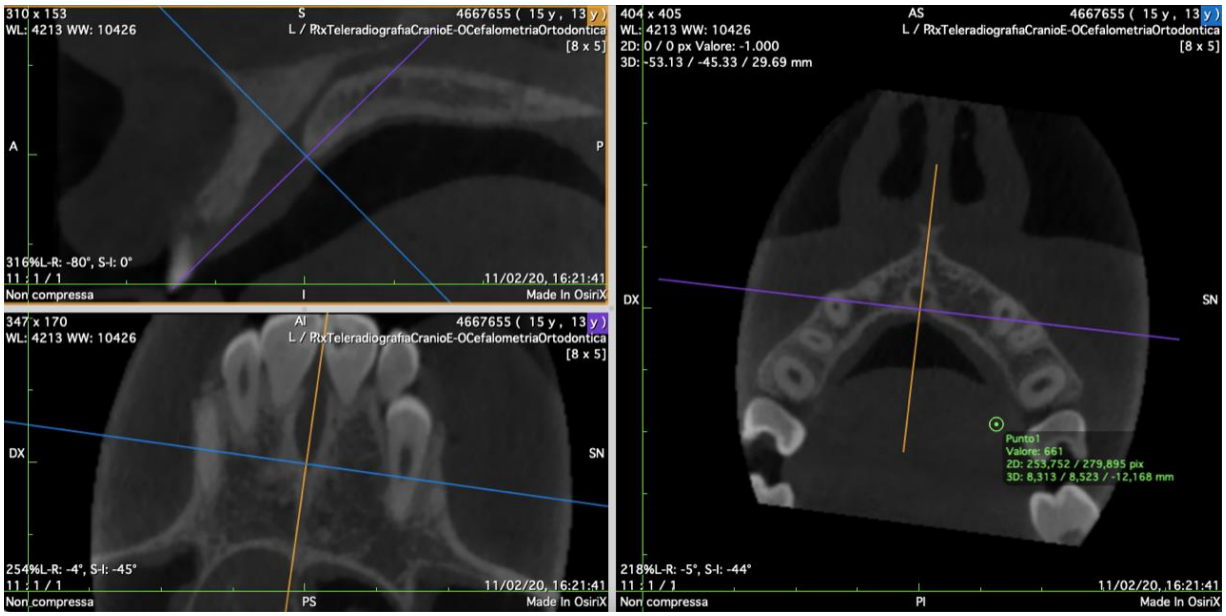

Figure 15 Before measurement, each site was oriented in all 3 planes of space. The sagittal axis was oriented according to the MPS, whereas the frontal and the transversal axes were oriented parallel and perpendicularly to the anterior palatine vault in the palatal rugae area in which the miniscrews are usually positioned. MPS; mid-palatal suture.

The nasopalatine foramen and the mid-palatal suture were selected as radiographic landmarks. A grid was devised, incorporating three lines located 3, 6, and 9 mm laterally and parallel to the midpalatal suture, as well as three perpendicular lines located 3, 6, and 9 mm dorsally to the posterior limit of the nasopalatine foramen, in agreement with previous research by Ludwig et al. The identical grid was overlaid on the nasal cortical plane (Figs. 16-17) [46].

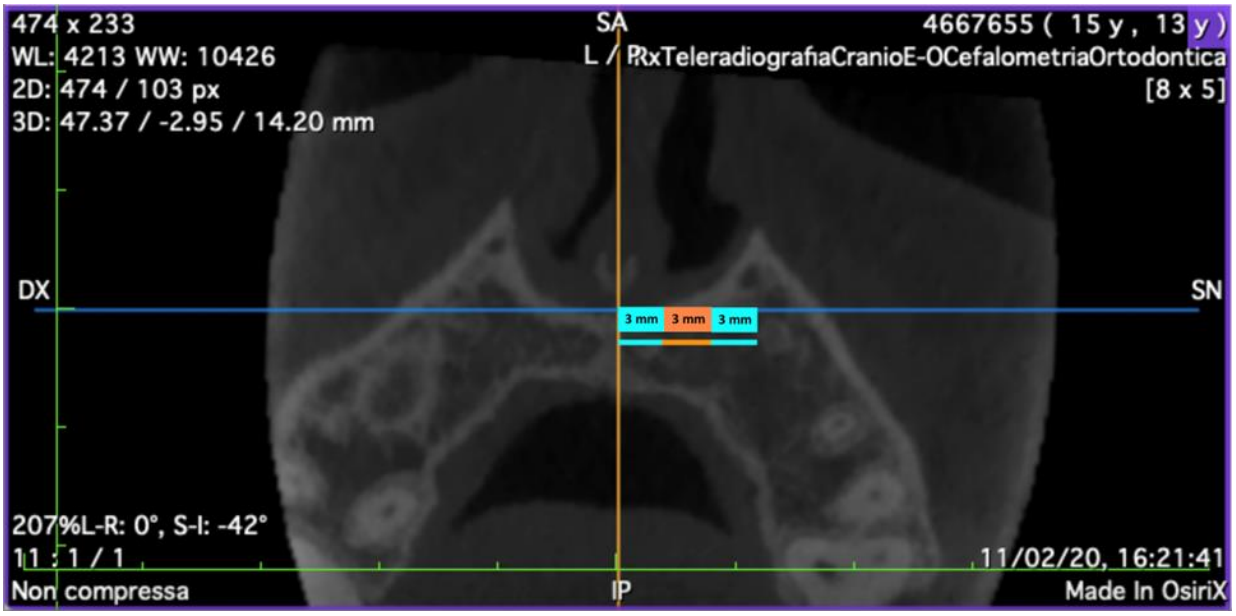

Figure 16: The axial slice defined 3 points 3, 6, and 9 mm to the midline. The sagittal slice was then moved 3, 6 and 9 mm.

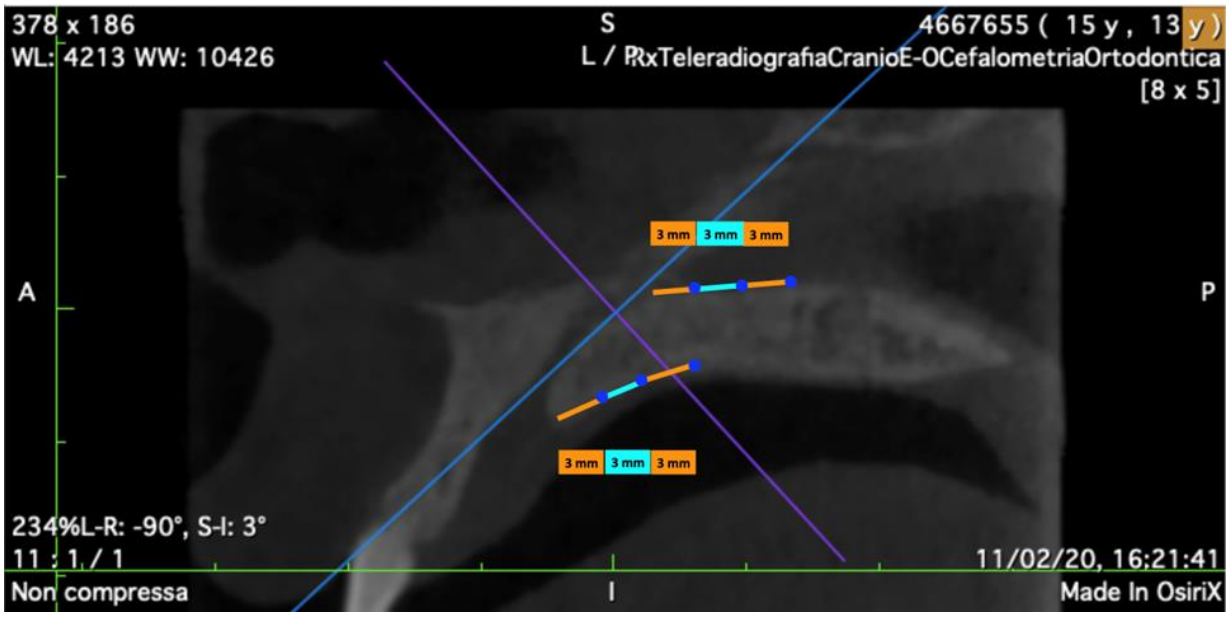

Figure 17: For each sagittal slice, points at 3, 6, and 9 mm dorsal to the nasopalatine foramen were evaluated on the oral and nasal cortical bones.

Intersecting points were evaluated, and bone density and thickness were measured at all nine points on the oral and nasal cortical bones. To address the non-uniformity of trabecular bone, medullary bone density was computed as the average bone density within a region of interest (ROI). The lines connecting the corresponding points on the two grids were delineated on the oral and nasal cortical plates, with software (Horos) calculating the mean bone density for each line (Fig. 18).

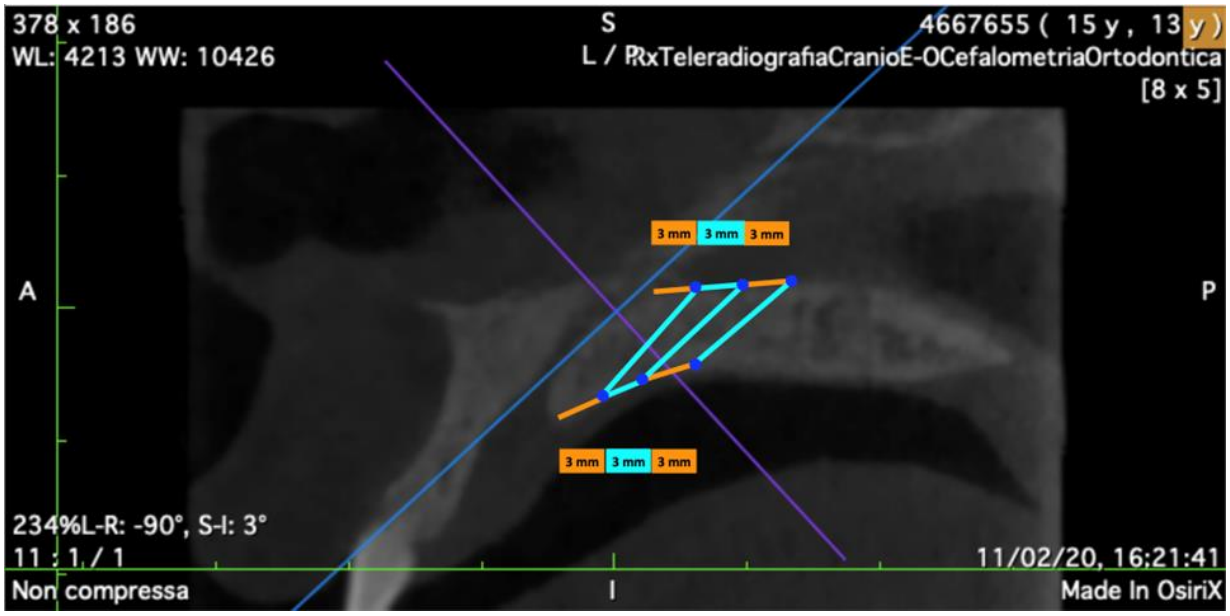

Figure 18: The software measured medullary bone density, which calculated the mean bone density (gray density units) in vertical lines through the corresponding points of the 2 grids.

Bone density was expressed in Gray Density Units, with all CBCT scans conducted using the same machine (Hyperion X9, My-Ray, Cefla s.c. 40026 Imola (Bo) Italy, www.my-ray.com) and identical settings for all patients. Furthermore, the Middle Phalanx Maturation method (MPM) stage was evaluated based on third finger middle phalanx radiographs according to the stages described by Perinetti et al [123] (Tab. 6).

Table 6: Description of the stages of the third finger middle phalanx maturation (MPM) method according to Perinetti et al (19).

Stage	Attainment
MPS1: The epiphysis is narrower or as wide as the metaphysis, but both lateral borders are tapered and rounded. Epiphysis and metaphysis are not fused.	More than 1 year before the peak of mandibular growth.
MPS2: epiphysis is at least as wide as the metaphysis with sides increasing thickness and showing a clear line of demarcation at right angle. In case of asymmetry between the two sides, the more mature side is used to assign the stage.	1 year before the mandibular growth peak.
MPS3: epiphysis is either as wide as or wider than the metaphysis with lateral sides showing an initial capping towards the metaphysis. Epiphysis and metaphysis are not fused.	Coincidental with the mandibular growth peak.
MPS4: The epiphysis begins to fuse with the metaphysis, but the contour is still recognizable.	After the mandibular growth peak.
MPS5: epiphysis is totally fused with the metaphysis.	At the end of pubertal growth spurt.

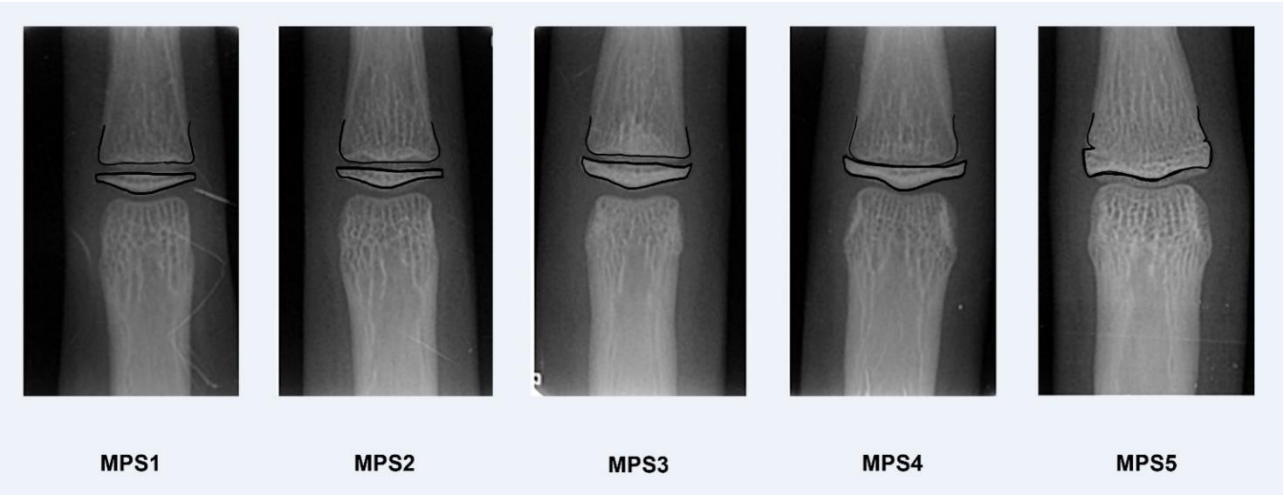

Figure 19: Clinical example of the stages of the third-finger MPM method according to Perinetti et al. [123] MPS, midpalatal suture; MPM, middle phalanx maturation.

Statistical analysis

A sample size of 11 subjects per group was determined to detect an effect size of 1.3 in the density of the the difference in palatal cortical between the MPS1-2-3 and MPS4-5 groups. After confirming the normality assumption using the Shapiro-Wilk test, intergroup differences between groups in the palatal and nasal cortical density, as well as medullary density, were evaluated using the independent sample t-test. Meanwhile, a one-way ANOVA with Tukey's correction examined the impact of skeletal maturation on palatal cortical and medullary density and nasal cortical density. The relationship between palatal and nasal cortical thickness and MPM stages was evaluated using a chi-square independence test, adopting a thickness threshold of 1 mm. To assess the significance of the difference between palatal and nasal cortical density across MPM stages, a paired-sample t-test was performed. Finally, the Pearson correlation coefficient was computed to correlate oral and nasal cortical density values with their respective values for the third finger middle phalanx. The significance level for all tests was established at 5%. Repeatability analysis was carried out on a randomly selected subset of 30 samples assessed at two different time points by two raters, employing the intraclass correlation coefficient (ICC) to determine inter- and intra-rater repeatability.

5.3.3 Results

Repeatability and Inter-rater Reliability

The intraclass correlation coefficient (ICC) demonstrates excellent intrarater repeatability for all measurements under analysis, with values of 0.96 (95% CI: 0.92-0.98) for oral cortical density, 0.97 (95% CI: 0.95-0.99) for nasal cortical density, 0.97 (95% CI: 0.96-0.98) for medullary density, and 0.93 (95% CI: 0.89-0.95) for cortical thickness. Inter-rater reliability also exhibits excellence, yielding ICC values of 0.96 (95% CI: 0.92-0.97) for oral cortical density, 0.97 (95% CI: 0.94-0.98) for nasal cortical density, 0.97 (95% CI: 0.96-0.98) for medullary density, and good reliability with a value of 0.86 (95% CI: 0.79-0.91) for cortical thickness.

Cortical Thickness Based on MPM Stage

Table 7 provides mean values, along with 95% confidence intervals, standard deviation, and minimum and maximum values for palatal and nasal cortical thickness, categorized by MPM stage (Tab. 7).

Table 7: Descriptive statistics for palatal and nasal cortical thickness divided according to MPM stage.

Variables	Mean	95% CI	SD	Min	Max
Palatal cortical thickness (mm)					
MPS1	0.98	0.88-1.07	0.14	0.84	1.31
MPS2	0.94	0.85-1.03	0.15	0.69	1.27
MPS3	0.92	0.80-1.05	0.20	0.75	1.47
MPS4	1.14	0.99-1.30	0.21	0.82	1.55
MPS5	1.11	0.95-1.27	0.26	0.74	1.60
Nasal cortical thickness (mm)					
MPS1	1.04	0.96-1.12	0.12	0.92	1.28
MPS2	0.95	0.87-1.03	0.13	0.77	1.27
MPS3	0.93	0.81-1.04	0.19	0.62	1.21
MPS4	1.07	0.95-1.18	0.15	0.81	1.35
MPS5	1.00	0.87-1.14	0.22	0.59	1.39

SD, standard deviation; MPS, midpalatal suture; MPM, middle phalanx maturation.

An examination of the relationship between MPM stages 1-2-3 and 4-5 and cortical thickness through the Chi-Square test reveals a significant association between the two variables, both for palatal cortical thickness ($X2$ (1, $N=60$) = 11.92, $p<0.001$) and nasal cortical thickness ($X2$ (1, $N=60$) = 4.26, $p<0.04$) as demonstrated in Table 8 (Tab. 8).

Table 8: Contingency tables for palatal and nasal cortical thickness grouping MPS stages 1-3 and 4 and 5 and using a thickness cutoff of 1 mm.

Variables		thickness		total
Palatal cortical thickness		<1	>1	
MPS1-2-3	count	25	12	37
	%	67.6%	32.4%	100%
MPS4-5	count	5	18	23
	%	21.7%	78.3%	100%
Total	count	30	30	60
	%	50.0%	50.0%	100%
Nasal cortical thickness				
MPS1-2-3	count	23	14	37
	%	62.16%	37.8%	100%
MPS4-5	count	8	15	23
	%	34.8%	65.2%	100%
Total	count	31	29	60
	%	51.7%	48.3%	100%

MPS, mid-palatal suture.

Effect of Skeletal Maturation on Palatal Cortical Density

ANOVA tests, assessing the influence of skeletal maturity, as determined by the MPM method, on mean palatal cortical density, indicate a statistically significant difference in mean density among at least two groups ($F(4,55) = [6.93]$, $p < 0.001$). Tukey's HSD Test for multiple comparisons further elucidates that the mean palatal cortical density is significantly different between MPS1 and MPS5 ($p = 0.001$, 95% C.I.= [-649.72, -125.53]), MPS2 and MPS5 ($p = 0.001$, 95% C.I.= [-620.98, -128.16]), and MPS3 and MPS5 ($p = 0.004$, 95% C.I.= [-594.74, -82.52]). However, no statistically significant differences in mean palatal cortical density were observed between the other stages, as detailed in Table 9 (Tab. 9).

Table 9: Descriptive statistics for palatal cortical density according to MPM stage

Variables	Mean	SD	95% C.I.	Min	Max
MPS1	1251.22	247.40	1085.02-1417.43	908.11	1620.67
MPS2	1264.28	167.35	1167.65-1360.91	987.55	1501.22
MPS3	1300.21	171.58	1191.20-1409.23	998.00	1643.89
MPS4	1485.85	217.70	1330.12-1641.59	1139.44	1900.55
MPS5	1638.85	303.25	1455.59-1822.10	1113.44	2096.89

SD, standard deviation; MPM, middle phalanx maturation; MPS, midpalatal suture.

An independent samples t-test highlights a significant disparity in palatal cortical density between stages MPS1-2-3 (M= 1272.05, SD= 191.13) and stages MPS4-5 (M= 1572.33, SD= 274.89); t(df)=58.00), p<0.001, as well as in palatal medullary density between stages MPS1-2-3 (M= 639.47, SD= 223.37) and stages MPS4-5 (M= 775.61, SD= 305.82); t(df)=58.00), p=0.05.

Skeletal Maturation and Nasal Cortical Density

Regarding the relationship between skeletal maturity, as measured by the MPM method, and mean nasal cortical density, a one-way ANOVA unveils a statistically significant difference in mean density between at least two groups (F (4,55) = [3.50], p=0.013). Tukey's HSD test for multiple comparisons discerns that the mean value of nasal cortical density is significantly different between MPS1 and MPS5 (p= 0.05, 95% CI = [-514.06, -0.27]) and between MPS2 and MPS5 (p= 0.007, 95% C.I.= [-542.99, -59.94]). However, no statistically significant differences in mean palatal cortical density were noted between the other stages, as elaborated in Table 10 (Tab. 10).

Table 10: Descriptive statistics for nasal cortical density according to MPM stage

Variables	Mean	SD	95% C.I.	Min	Max
MPS1	1424.13	153.32	1321.13-1527.13	1112.78	1645.44
MPS2	1379.83	182.96	1274.19-1485.47	996.89	1675.33
MPS3	1488.01	248.48	1330.13-1645.88	1034.33	1990.55
MPS4	1489.63	112.18	1409.38-1569.88	1305.44	1633.11
MPS5	1681.30	323.56	1485.77-1876.82	1156.11	2237.00

SD, standard deviation; MPM, middle phalanx maturation; MPS, midpalatal suture.

An independent samples t-test reveals a significant discrepancy in nasal cortical density between stages MPS1-2-3 (M= 1428.09, SD= 198.97) and stages MPS4-5 (M= 1597.97, SD= 267.75); t(df)=58.00), $p<0.001$.

Effect of Skeletal Maturation on Palatal Medullary Density

When appraising the effect of skeletal maturity, as assessed through the MPM method, on the mean density of palatal medullary bone, ANOVA tests do not reveal statistically significant differences in mean density between any of the groups, as presented in Table 11 (Tab. 11).

Table 11: Descriptive statistics for palatal medullary density according to MPM stage

Variables	Mean	SD	95% C.I.	Min	Max
MPS1	639.64	214.14	495.78-783.49	320.22	881.00
MPS2	571.01	201.90	454.44-687.59	200.44	978.22
MPS3	719.18	246.02	562.86-875.49	318.00	989.11
MPS4	722.64	274.30	526.42-918.87	360.11	1189.78
MPS5	816.35	333.01	615.11-1017.59	378.00	1539.78

SD, standard deviation; MPM, middle phalanx maturation; MPS, midpalatal suture

Correlation Between Cortical Density and MPM Stages

The Pearson correlation coefficient indicates a positive correlation between oral and nasal cortical density and MPM stages (oral cortical density: $r(58)= .54$, $p<0.001$; nasal cortical density: $r(58)= .39$, $p= 0.002$).

Differences in Palatal and Nasal Cortical Density

Lastly, paired sample t-tests detect a significant difference in mean density between the palatal cortical and the nasal cortical for stage MPS1 (palatal: M=1251.22, SD= 247.40; nasal: 1424.13, SD= 153.32) ($p= 0.05$), MPS2 (palatal: M=1264.28, SD= 167.36; nasal: M=1379.83, SD=182.96) ($p<0.001$); and MPS3 (palatal: M=1300.21, SD= 171.58; nasal: M=1488.01, SD= 148.48) ($p=0.03$). No statistical differences were found for stages MPS4 and MPS5. (Fig. 20).

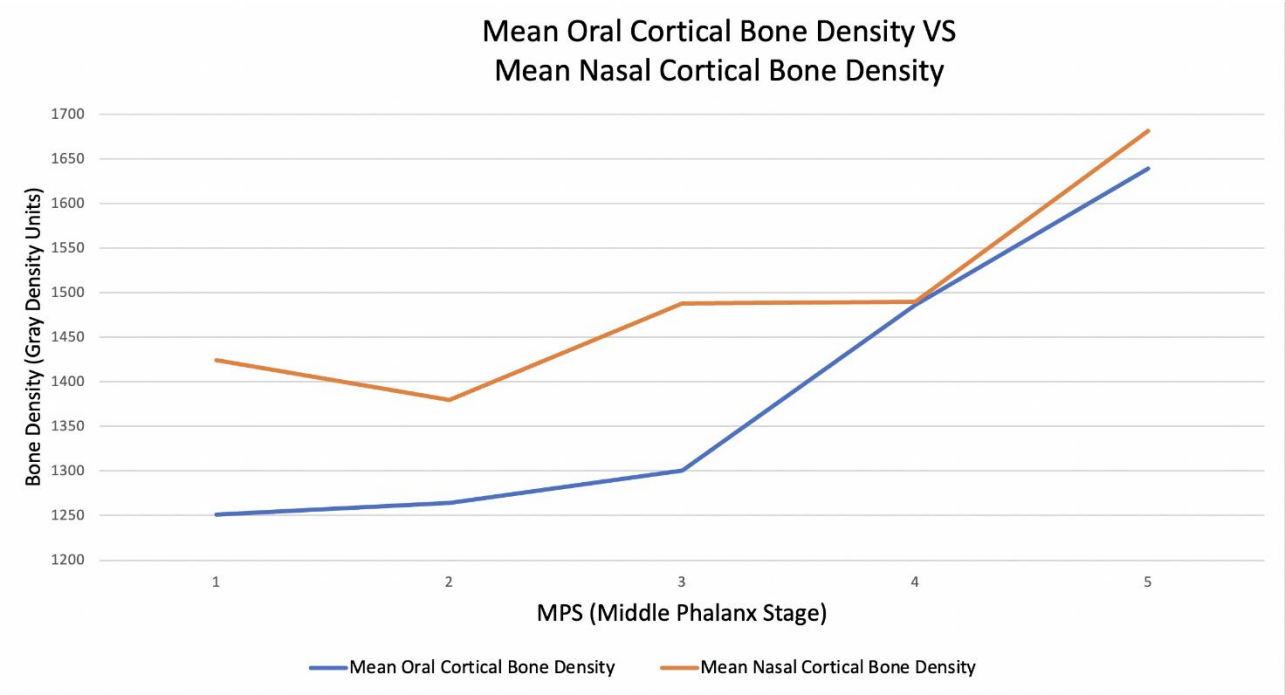

Figure 20: Mean oral cortical bone density vs. mean nasal cortical bone density (gray density units)

5.3.4 Discussion and Conclusions

Bone quality plays a crucial role in the success of dental implants and miniscrews. Parameters such as bone density and cortical thickness are recognized as pivotal factors contributing to primary stability during implantation processes [35, 128-130]. Computed Tomography (CT) scans are routinely employed for quantitative and qualitative assessment of bone quality before surgical procedures. The Hounsfield unit (HU) is a widely used parameter for the objective determination of bone density [131]. The advent of Cone Beam Computed Tomography (CBCT) imaging has brought significant advances in oral and maxillofacial imaging. This technology offers notable benefits, including superior spatial resolution, dimensional accuracy, and enhanced gray density range and contrast, while delivering reduced radiation doses compared to conventional CT scans [131, 132]. However, it should be noted that, unlike CT, gray density values in CBCT images, also called voxel values (VV), are not universally standardized and can vary across different X-ray devices [132]. Consequently, these values should be interpreted with caution. In the present study, CBCT scans were obtained using the same CBCT unit, allowing a qualitative evaluation of bone density trends in various maturation stages. It is important to note that to date, the literature lacks a reference value in CT HU that can reliably predict the primary stability of miniscrews. Cortical thickness has been closely associated with achieving primary stability for miniscrews and implants [36, 133-135]. Specifically, a cortical bone thickness of at least 1 mm has been identified as a critical factor for ensuring primary stability and is considered sufficient for this purpose by some researchers [136]. Furthermore, numerous studies have established correlations between primary stability and cortical, as well as cancellous, bone density [137]. In the current study, the thickness of the palatal and nasal cortical was measured and categorized according to the patient's MPM stage, ranging from 1 to 5 (Tab. 6). In particular, the mean thickness of the palatal cortical was less than 1 mm in stages MPS1, MPS2, and

MPS3, while it exceeded 1 mm in stages MPS4 and MPS5. Similar trends were observed for mean nasal cortical thickness. These findings align with the trends in bone mineral accrual seen in growing patients [138, 139] and correspond to clinical observations of increased skeletal maturation in post-pubertal subjects (MPS4 and MPS5), whereas prepubertal individuals (MPS1 and MPS2) and early pubertal subjects (MPS3) typically exhibit lower levels of skeletal growth. To assess cortical thickness based on varying levels of skeletal maturation between prepubertal and post-pubertal patients, a grouping was performed, considering stages MPS1-2-3 and MPS4-5 (Tab. 7). Among patients in MPS1-2-3, 67.6% had a mean palatal cortical thickness of less than 1 mm, while 78.3% of patients in stages MPS4-5 had a mean palatal cortical thickness greater than 1 mm. A similar trend was observed for nasal cortical thickness, with a lower disparity between MPS1-2-3 stages (62.16% < 1 mm) and MPS4-5 (65.2% > 1 mm). Mean densities of the palatal and nasal cortical regions were also evaluated using gray units as the unit of measurement. Mean values were determined for patients in MPM stages 1 to 5 (Tab. 8). The palatal cortical density showed an increasing trend from MPS1 to MPS5. Notably, MPS1, MPS2, and MPS3 exhibited similar values, whereas MPS4 demonstrated a significant increase, and MPS5 presented even higher values. A significant difference in palatal cortical density was found between stages MPS1-2-3 (M= 1272.05, SD= 191.13) and stages MPS4-5 (M= 1572.33, SD= 274.89); $p<0.001$. These results again align with trends in bone mineral accrual during growth [138, 139] and with clinical observations of greater skeletal maturation in post-pubertal subjects (MPS4 and MPS5). The nasal cortical density exhibited similar values in MPS1, MPS2, MPS3, and MPS4, with a significant increase observed in MPS5 (Tab. 10). A significant difference in nasal cortical density was observed between stages MPS1-2-3 (M= 1428.09, SD= 198.97) and stages MPS4-5 (M= 1597.97, SD= 267.75); $p<0.001$. Palatal medullary density was also assessed (Tab. 11). This measurement showed substantial standard deviation values, reflecting considerable variation in values among patients within the same stage of MPS and even within the same patient. A one-way analysis of variance (ANOVA) test did not reveal statistically significant differences in mean density between any of the groups. A comparison of mean palatal and nasal cortical density was performed for each MPS stage (Fig. 20). Significant differences were observed in stages MPS1, MPS2, and MPS3 ($p<0.05$), while no statistically significant differences were found for stages MPS4 and MPS5.

Several potential limitations of the study must be acknowledged. Notably, the study did not group patients based on sex or skeletal type (brachyfacial vs. dolichofacial), which could influence results, especially in post-pubertal patients. Additionally, future investigations could explore these differences. Furthermore, bone density was measured in Gray Density Units, a nonstandardized unit, which limits direct comparisons with other values in the literature. However, given that all CBCT scans were obtained using the same device, a qualitative assessment of bone density trends across different maturation stages was still feasible. Lastly, as mentioned earlier, the literature lacks CT HU reference values to predict the primary stability.

The study results carry significant clinical implications. The substantial increase in palatal cortical thickness and density observed in MPS4 and 5 suggests a higher likelihood of primary stability in these patients. Conversely, patients in stages MPS1, MPS2, and MPS3

may experience a lower success rate due to the thinner and lower-quality palatal cortical bone. To mitigate the risk of miniscrew failure in MPS1-2-3 individuals with inferior palatal cortical bone characteristics, bicortical insertion could be considered, particularly when greater orthodontic forces are required. It is worth noting that cortical drilling does not seem advisable, as it may increase the risk of failure in these patients.

On the contrary, bicortical insertion can pose challenges during miniscrew placement, especially in late adolescents and young adults, due to the high insertion torque required. This clinical observation is in line with the study findings, which revealed higher cortical bone densities in the palatal (1639.85 ± 303.25) and nasal (1681.30 ± 323.56) in MPS5 patients. Since the thickness and density of nasal cortical bone have not been extensively investigated in the literature, these findings suggest a potential need to revise miniscrew designs and insertion techniques in MPS5 patients who require bicortical insertion.

Furthermore, the results may have broader implications for the planning of orthodontic treatment, which extend beyond miniscrew insertion. For example, the lower cortical bone density observed in MPS1-2-3 individuals could support earlier intervention in the treatment of impacted teeth, thus preventing the development of abnormal root morphology resulting from alveolar bone obstruction.

Conclusions

In summary:

- MPS1, MPS2 and MPS3 exhibit lower palatal cortical bone density and thickness, with higher nasal cortical bone density.
- MPS4 and MPS5 display higher palatal and nasal cortical bone density and thickness, with MPS5 showing the highest values across all variables.
- Medullary bone density shows substantial standard deviation values, reflecting considerable variation and no definitive conclusions could be drawn from the data.

6 GENERAL DISCUSSION AND CONCLUSIONS

This PhD dissertation aimed to investigate and analyze protocols for the insertion of palatal miniscrews, with the objective of synthesizing, assessing, and enhancing optimal strategies for effectively utilizing palatal anchorage in conjunction with digital technologies. The long-term goal was to establish a set of guidelines for the proficient management of all pertinent variables associated with the one- and two-visit protocols.

Existing literature already underscores the preference for bicortical insertion when substantial anchorage is requisite, particularly in the context of Miniscrews-Assisted Rapid Palatal Expansion (MARPE) in adult patients. This is recommended to achieve a more extensive and parallel expansion while mitigating the risk of mini-screw failure. However, after scrutinizing the thickness and density of the palatal and nasal cortical bone, it has been observed that bicortical engagement may also enhance the stability of the miniscrew in prepubertal patients, where the palatal cortical bone exhibits reduced thickness and density. Conversely, given the superior bone quality in young adults and the subsequent elevated insertion torque necessitated by bicortical insertion, miniscrews that do not require palatal expansion may represent a safer option for monocortical insertion.

Regarding operational protocols, our findings have prompted the suggestion of a two-visit protocol for any device supported by four mini-screws. The structural demands and constraints imposed by such devices heighten concerns of protocol failure under a one-visit approach. Conversely, a one-visit protocol can be effectively employed for devices supported by two mini-screws.

To enhance the effectiveness and efficiency of the one-visit protocol, particularly when working with more than two miniscrews, it is recommended to enlist the assistance of an additional individual to stabilize the surgical guide during the procedure and to employ a pilot hole.

Future research endeavors will concentrate on discerning the variance in failure rates between monocortical and bicortical mini-screws and the distinctions in miniscrew migration among various device types and cortical engagement strategies.

7 REFERENCES

1. Ure DS, Oliver DR, Kim KB, Melo AC, Buschang PH. Stability changes of miniscrew implants over time. Angle Orthod. Nov 2011;81(6):994-1000. doi:10.2319/120810-711.1
2. Baumrind S. A reconsideration of the propriety of the "pressure-tension" hypothesis. Am J Orthod. Jan 1969;55(1):12-22. doi:10.1016/s0002-9416(69)90170-5
3. Proffit W, Fields, HW., & Sarver, DM. Contemporary Orthodontics. 2013.
4. Nanda R, Sumit Y. Temporary Anchorage Devices in Orthodontics. 2nd edition ed. 2019.
5. Feldmann I, Bondemark L. Orthodontic anchorage: a systematic review. Angle Orthod. May 2006;76(3):493-501. doi:10.1043/0003-3219(2006)076[0493:Oa]2.0.Co;2
6. Moyers R. Force systems and rissue responses to forces in orthodontics and facial orthopedics. In: Publishers LYBM, ed. Handbook of Orthodontics. 1988:309.
7. Sivakrishna P, Prasad, M., Ava, Singaraju, G.S., & Ganugapanta, V. Anchorage in orthodontics: a literature review. Annals and essences of dentistry. 2016;8:7-19.

8. Jepsen A. Root surface measurement and a method for x-ray determination of root surface area. Acta Odontol Scand. 1963 Feb;21:35-46. doi: 10.3109/00016356309019777. PMID: 13961805.

9. Nahidh M, Al Azzawi, AM., & Al-Badri, SC. Understanding anchorage in orthodontics. J Dent Oral Disord. 2019;5(2):1117.
10. Ganzer N, Feldmann I, Petrén S, Bondemark L. A cost-effectiveness analysis of anchorage reinforcement with miniscrews and molar blocks in adolescents: a randomized controlled trial. Eur J Orthod. 2019 Mar 29;41(2):180-187. doi: 10.1093/ejo/cjy041. PMID: 30668660.
11. Roberts W, Garetto, LP., & Simmons, KE. Principles of orthodontic biomechanics; metabolic and mechanical control mechanisms. In: Ann Arbor UoMP, ed. Bone biodynamics in orthodontic and orthopedic treatment. 1992:189-225.
12. D Diar-Bakirly S, Feres MF, Saltaji H, Flores-Mir C, El-Bialy T. Effectiveness of the transpalatal arch in controlling orthodontic anchorage in maxillary premolar extraction cases: A systematic review and meta-analysis. Angle Orthod. 2017 Jan;87(1):147-158. doi: 10.2319/021216-120.1. Epub 2016 Aug 9. PMID: 27504820; PMCID: PMC8388582.
13. Almuzian M, Alharbi F, McIntyre G. Extra-oral appliances in orthodontic treatment. Dent Update. Jan-Feb 2016;43(1):74-6, 79-82. doi:10.12968/denu.2016.43.1.74
14. Kokich VG, Shapiro PA, Oswald R, Koskinen-Moffett L, Clarren SK. Ankylosed teeth as abutments for maxillary protraction: a case report. Am J Orthod. 1985 Oct;88(4):303-7. doi: 10.1016/0002-9416(85)90129-0. PMID: 3901773.
15. Gainsforth BL, & Higley, L. A study of orthodontic anchorage possibilities in basal bone. American Journal of Orthodontics and Oral Surgery. 1945;31:406-417.

16. Roberts WE, Smith RK, Zilberman Y, Mozsary PG, Smith RS. Osseous adaptation to continuous loading of rigid endosseous implants. Am J Orthod. 1984 Aug;86(2):95-111. doi: 10.1016/0002-9416(84)90301-4. PMID: 6589962.
17. Creekmore TD, Eklund MK. The possibility of skeletal anchorage. J Clin Orthod. Apr 1983;17(4):266-9.
18. Tettamanti L, Andrisani C, Bassi MA, Vinci R, Silvestre-Rangil J, Tagliabue A. Immediate loading implants: review of the critical aspects. Oral Implantol (Rome). Apr-Jun 2017;10(2):129-139. doi:10.11138/orl/2017.10.2.129
19. Wehrbein H, Glatzmaier J, Mundwiller U, Diedrich P. Das Orthosystem — Ein neues Implantatsystem zur orthodontischen Verankerung am Gaumen. Journal of Orofacial Orthopedics / Fortschritte der Kieferorthopädie. 1996/06/01 1996;57(3):142-153. doi:10.1007/BF02191878
20. Kanomi R. Mini-implant for orthodontic anchorage. J Clin Orthod. Nov 1997;31(11):763-7.
21. Block MS, Hoffman DR. A new device for absolute anchorage for orthodontics. Am J Orthod Dentofacial Orthop. 1995 Mar;107(3):251-8. doi: 10.1016/s0889-5406(95)70140-0. PMID: 7879757.
22. Freudenthaler JW, Haas R, Bantleon HP. Bicortical titanium screws for critical orthodontic anchorage in the mandible: a preliminary report on clinical applications. Clin Oral Implants Res. 2001 Aug;12(4):358-63. English, French, German. doi: 10.1034/j.1600-0501.2001.012004358.x. PMID: 11488865.
23. Chang HP, Tseng YC. Miniscrew implant applications in contemporary orthodontics. Kaohsiung J Med Sci. Mar 2014;30(3):111-5. doi:10.1016/j.kjms.2013.11.002
24. Paik C. Orthodontic Miniscrew Implants: Clinical Applications. 2009:23-24.
25. Noble J. Evidence Based use of Orthodontic TSADs. In Evidence-based clinical orthodontics. Quintessance; 2012:107-126.
26. Brettin BT, Grosland NM, Qian F, Southard KA, Stuntz TD, Morgan TA, Marshall SD, Southard TE. Bicortical vs monocortical orthodontic skeletal anchorage. Am J Orthod Dentofacial Orthop. 2008 Nov;134(5):625-35. doi: 10.1016/j.ajodo.2007.01.031. PMID: 18984394.
27. Ishii T, Nojima K, Nishii Y, Takaki T, Yamaguchi H. Evaluation of the implantation position of mini-screws for orthodontic treatment in the maxillary molar area by a micro CT. Bull Tokyo Dent Coll. 2004 Aug;45(3):165-72. doi: 10.2209/tdcpublication.45.165. PMID: 15779459.
28. Park H. An anatomical study using CT images for the implantation of micro-implants. Korean J Orthod. 2002;32(6):435-441.
29. Rozé J, Babu S, Saffarzadeh A, Gayet-Delacroix M, Hoornaert A, Layrolle P. Correlating implant stability to bone structure. Clin Oral Implants Res. Oct 2009;20(10):1140-5. doi:10.1111/j.1600-0501.2009.01745.x

30. Brinley CL, Behrents R, Kim KB, Condoor S, Kyung HM, Buschang PH. Pitch and longitudinal fluting effects on the primary stability of miniscrew implants. Angle Orthod. Nov 2009;79(6):1156-61. doi:10.2319/103108-554r.1
31. Motoyoshi M, Hirabayashi M, Uemura M, Shimizu N. Recommended placement torque when tightening an orthodontic mini-implant. Clinical Oral Implants Research. 2006;17(1):109-114. doi:https://doi.org/10.1111/j.1600-0501.2005.01211.x
32. Marquezan M, Mattos CT, Sant'Anna EF, de Souza MM, Maia LC. Does cortical thickness influence the primary stability of miniscrews?: A systematic review and meta-analysis. Angle Orthod. Nov 2014;84(6):1093-103. doi:10.2319/093013-716.1
33. Marquezan M, Lima I, Lopes RT, Sant'Anna EF, de Souza MM. Is trabecular bone related to primary stability of miniscrews? Angle Orthod. May 2014;84(3):500-7. doi:10.2319/052513-39.1
34. Pan CY, Liu PH, Tseng YC, Chou ST, Wu CY, Chang HP. Effects of cortical bone thickness and trabecular bone density on primary stability of orthodontic mini-implants. J Dent Sci. 2019 Dec;14(4):383-388. doi: 10.1016/j.jds.2019.06.002. Epub 2019 Jul 20. PMID: 31890126; PMCID: PMC6921117.
35. Papageorgiou SN, Zogakis IP, Papadopoulos MA. Failure rates and associated risk factors of orthodontic miniscrew implants: a meta-analysis. Am J Orthod Dentofacial Orthop. 2012 Nov;142(5):577-595.e7. doi: 10.1016/j.ajodo.2012.05.016. PMID: 23116500.
36. Motoyoshi M, Inaba M, Ono A, Ueno S, Shimizu N. The effect of cortical bone thickness on the stability of orthodontic mini-implants and on the stress distribution in surrounding bone. Int J Oral Maxillofac Surg. Jan 2009;38(1):13-8. doi:10.1016/j.ijom.2008.09.006
37. Farnsworth D, Rossouw PE, Ceen RF, Buschang PH. Cortical bone thickness at common miniscrew implant placement sites. Am J Orthod Dentofacial Orthop. 2011 Apr;139(4):495-503. doi: 10.1016/j.ajodo.2009.03.057. PMID: 21457860.
38. Melsen B, Costa A. Immediate loading of implants used for orthodontic anchorage. Clin Orthod Res. Feb 2000;3(1):23-8. doi:10.1034/j.1600-0544.2000.030105.x
39. Meredith N. Assessment of implant stability as a prognostic determinant. Int J Prosthodont. Sep-Oct 1998;11(5):491-501.
40. Lim HJ, Eun CS, Cho JH, Lee KH, Hwang HS. Factors associated with initial stability of miniscrews for orthodontic treatment. Am J Orthod Dentofacial Orthop. 2009 Aug;136(2):236-42. doi: 10.1016/j.ajodo.2007.07.030. PMID: 19651354.
41. Chen Y, Kyung HM, Zhao WT, Yu WJ. Critical factors for the success of orthodontic mini-implants: a systematic review. Am J Orthod Dentofacial Orthop. Mar 2009;135(3):284-91. doi:10.1016/j.ajodo.2007.08.017
42. Maino BG, Mura P, Bednar J. Miniscrew implants: The Spider Screw anchorage system. Seminars in Orthodontics. 2005/03/01/ 2005;11(1):40-46. doi:https://doi.org/10.1053/j.sodo.2004.11.007
43. Ghislanzoni LH, Berardinelli F, Ludwig B, Lucchese A. Considerations Involved in Placing Miniscrews Near the Nasopalatine Bundle. J Clin Orthod. May 2016;50(5):321-8.
44. Park H. linical study on success rate of microscrew implants for orthodontic anchorage. Korean J Orthod. 2003;33(3):151-156.

45. Wilmes B, Drescher D, Nienkemper M. A miniplate system for improved stability of skeletal anchorage. J Clin Orthod. Aug 2009;43(8):494-501.
46. Ludwig B, Glasl B, Bowman SJ, Wilmes B, Kinzinger GS, Lisson JA. Anatomical guidelines for miniscrew insertion: palatal sites. J Clin Orthod. Aug 2011;45(8):433-41; quiz 467.
47. Kang S, Lee SJ, Ahn SJ, Heo MS, Kim TW. Bone thickness of the palate for orthodontic mini-implant anchorage in adults. Am J Orthod Dentofacial Orthop. 2007 Apr;131(4 Suppl):S74-81. doi: 10.1016/j.ajodo.2005.09.029. PMID: 17448390.
48. Gracco A, Lombardo L, Cozzani M, Siciliani G. Quantitative evaluation with CBCT of palatal bone thickness in growing patients. Prog Orthod. 2006;7(2):164-74.
49. Ryu JH, Park JH, Vu Thi Thu T, Bayome M, Kim Y, Kook YA. Palatal bone thickness compared with cone-beam computed tomography in adolescents and adults for mini-implant placement. Am J Orthod Dentofacial Orthop. 2012 Aug;142(2):207-12. doi: 10.1016/j.ajodo.2012.03.027. PMID: 22858330.
50. Kim YH, Yang SM, Kim S, Lee JY, Kim KE, Gianelly AA, Kyung SH. Midpalatal miniscrews for orthodontic anchorage: factors affecting clinical success. Am J Orthod Dentofacial Orthop. 2010 Jan;137(1):66-72. doi: 10.1016/j.ajodo.2007.11.036. PMID: 20122433.
51. Park J. Temporary anchorage devices in clinical orthodontics. 2020.
52. King KS, Lam EW, Faulkner MG, Heo G, Major PW. Vertical bone volume in the paramedian palate of adolescents: a computed tomography study. Am J Orthod Dentofacial Orthop. 2007 Dec;132(6):783-8. doi: 10.1016/j.ajodo.2005.11.042. PMID: 18068597.
53. Kravitz ND, Kusnoto B. Risks and complications of orthodontic miniscrews. Am J Orthod Dentofacial Orthop. 2007/04/01/ 2007;131(4, Supplement):S43-S51. doi:https://doi.org/10.1016/j.ajodo.2006.04.027
54. Holberg C, Winterhalder P, Rudzki-Janson I, Wichelhaus A. Finite element analysis of mono- and bicortical mini-implant stability. Eur J Orthod. 2014 Oct;36(5):550-6. doi: 10.1093/ejo/cjt023. Epub 2013 Apr 18. PMID: 23598610.
55. Holberg C, Winterhalder P, Holberg N, Rudzki-Janson I, Wichelhaus A. Direct versus indirect loading of orthodontic miniscrew implants-an FEM analysis. Clin Oral Investig. 2013 Nov;17(8):1821-7. doi: 10.1007/s00784-012-0872-4. Epub 2012 Oct 31. PMID: 23111639.

56. Li N, Sun W, Li Q, Dong W, Martin D, Guo J. Skeletal effects of monocortical and bicortical mini-implant anchorage on maxillary expansion using cone-beam computed tomography in young adults. Am J Orthod Dentofacial Orthop. 2020 May;157(5):651-661. doi: 10.1016/j.ajodo.2019.05.021. Erratum in: Am J Orthod Dentofacial Orthop. 2020 Sep;158(3):318. PMID: 32354438.
57. Perinetti G, Bruno, A., & Tonini, P. Ancoraggio palatale: istruzioni per l'uso. Bollettino di Informazione Leone. 2020;106:38-51.

58. Leung MT, Lee TC, Rabie AB, Wong RW. Use of miniscrews and miniplates in orthodontics. J Oral Maxillofac Surg. 2008 Jul;66(7):1461-6. doi: 10.1016/j.joms.2007.12.029. PMID: 18571031.
59. Wilmes B, Nienkemper M, Drescher D. Application and effectiveness of a mini-implant- and tooth-borne rapid palatal expansion device: the hybrid hyrax. World J Orthod. Winter 2010;11(4):323-30.
60. Di Leonardo B, Ludwig B, Glasl B, Hourfar J, Mura R. BRÖLEX - Eine rein knochengetragene Expansionsapparatur.
61. Perinetti G, Dal Borgo, B., Contardo, L., Bruno, A., & Tonini, P. MaXimo: un nuovo distalizzatore intraorale ancorato su miniviti palatali. Bollettino di Informazione Leone. 2016;98:54-62.

62. Wilmes B, Nienkemper M, Ludwig B, Nanda R, Drescher D. Upper-molar intrusion using anterior palatal anchorage and the Mousetrap appliance. J Clin Orthod. May 2013;47(5):314-20; quiz 328.
63. Kılınç DD, Sayar G. Various Contemporary Intraoral Anchorage Mechanics Supported with Temporary Anchorage Devices. Turk J Orthod. Dec 2016;29(4):109-113. doi:10.5152/TurkJOrthod.2016.16027
64. Mullen SR, Martin CA, Ngan P, Gladwin M. Accuracy of space analysis with emodels and plaster models. Am J Orthod Dentofacial Orthop. 2007 Sep;132(3):346-52. doi: 10.1016/j.ajodo.2005.08.044. PMID: 17826603.
65. Sousa MV, Vasconcelos EC, Janson G, Garib D, Pinzan A. Accuracy and reproducibility of 3-dimensional digital model measurements. Am J Orthod Dentofacial Orthop. 2012 Aug;142(2):269-73. doi: 10.1016/j.ajodo.2011.12.028. PMID: 22858338.
66. Camardella LT, Breuning H, de Vasconcellos Vilella O. Accuracy and reproducibility of measurements on plaster models and digital models created using an intraoral scanner. J Orofac Orthop. 2017 May;78(3):211-220. English. doi: 10.1007/s00056-016-0070-0. Epub 2017 Jan 10. PMID: 28074260.
67. Asquith J, Gillgrass T, Mossey P. Three-dimensional imaging of orthodontic models: a pilot study. Eur J Orthod. 2007 Oct;29(5):517-22. doi: 10.1093/ejo/cjm044. PMID: 17974542.
68. Shastry S, Park JH. Evaluation of the use of digital study models in postgraduate orthodontic programs in the United States and Canada. Angle Orthod. 2014 Jan;84(1):62-7. doi: 10.2319/030813-197.1. Epub 2013 Jun 6. PMID: 23742197; PMCID: PMC8683047.
69. Graf S, Hansa I. Clinical guidelines to integrate temporary anchorage devices for bone-borne orthodontic appliances in the digital workflow. APOS Trends in Orthodontics. 9doi:10.25259/APOS_78_2019
70. Richert R, Goujat A, Venet L, Viguie G, Viennot S, Robinson P, Farges JC, Fages M, Ducret M. Intraoral Scanner Technologies: A Review to Make a Successful Impression. J Healthc Eng. 2017;2017:8427595. doi: 10.1155/2017/8427595. Epub 2017 Sep 5. PMID: 29065652; PMCID: PMC5605789.
71. Wiranto MG, Engelbrecht WP, Tutein Nolthenius HE, van der Meer WJ, Ren Y. Validity, reliability, and reproducibility of linear measurements on digital models obtained from intraoral and cone-beam computed tomography scans of alginate impressions. Am J Orthod Dentofacial Orthop. Jan 2013;143(1):140-7. doi:10.1016/j.ajodo.2012.06.018
72. Grauer D, Proffit WR. Accuracy in tooth positioning with a fully customized lingual orthodontic appliance. Am J Orthod Dentofacial Orthop. 2011 Sep;140(3):433-43. doi: 10.1016/j.ajodo.2011.01.020. PMID: 21889089.
73. Iodice G, Nanda R, Drago S, Repetto L, Tonoli G, Silvestrini-Biavati A, Migliorati M. Accuracy of direct insertion of TADs in the anterior palate with respect to a 3D-assisted digital insertion virtual planning. Orthod Craniofac Res. 2022 May;25(2):192-198. doi: 10.1111/ocr.12525. Epub 2021 Aug 9. PMID: 34344059.74. Perinetti G, Bruno, A., & Tonini, P. Inserzione guidata di miniviti ortodontiche: il sistema di pianificazione "REPLICA". Il nuovo laboratorio odontotecnico. 2020:23-33.
75. Jung BA, Wehrbein H, Heuser L, Kunkel M. Vertical palatal bone dimensions on lateral cephalometry and cone-beam computed tomography: implications for palatal implant placement. Clin Oral Implants Res. 2011 Jun;22(6):664-8. doi: 10.1111/j.1600-0501.2010.02021.x. Epub 2010 Oct 6. PMID: 21044170.
76. Cantarella D, Savio G, Grigolato L, Zanata P, Berveglieri C, Lo Giudice A, Isola G, Del Fabbro M, Moon W. A new methodology for the digital planning of micro-implant-supported maxillary skeletal expansion. Med Devices (Auckl). 2020 Mar 18;13:93-106. doi: 10.2147/MDER.S247751. PMID: 32256130; PMCID: PMC7090180.
77. Sánchez-Riofrío D, Viñas MJ, Ustrell-Torrent JM. CBCT and CAD-CAM technology to design a minimally invasive maxillary expander. BMC Oral Health. 2020/11/04 2020;20(1):303. doi:10.1186/s12903-020-01292-3
78. Cantarella D, Quinzi V, Karanxha L, Zanata P, Savio G, Del Fabbro M. Digital Workflow for 3D Design and Additive Manufacturing of a New Miniscrew-Supported Appliance for Orthodontic Tooth Movement. Applied Sciences. 2021;11(3):928.
79. Francisco I, Ribeiro MP, Marques F, Travassos R, Nunes C, Pereira F, Caramelo F, Paula AB, Vale F. Application of Three-Dimensional Digital Technology in Orthodontics: The State of the Art. Biomimetics (Basel). 2022 Feb 2;7(1):23. doi: 10.3390/biomimetics7010023. PMID: 35225915; PMCID: PMC8883890.
80. Möhlhenrich SC, Brandt M, Kniha K, Prescher A, Hölzle F, Modabber A, Wolf M, Peters F. Accuracy of orthodontic mini-implants placed at the anterior palate by tooth-borne or gingiva-borne guide support: a cadaveric study. Clin Oral Investig. 2019 Dec;23(12):4425-4431. doi: 10.1007/s00784-019-02885-1. Epub 2019 Apr 13. PMID: 30982181.

81. Cassetta M, Giansanti M. Accelerating orthodontic tooth movement: A new, minimally-invasive corticotomy technique using a 3D-printed surgical template. Med Oral Patol Oral Cir Bucal. Jul 1 2016;21(4):e483-7. doi:10.4317/medoral.21082
82. Cassetta M, Altieri F, Di Giorgio R, Barbato E. Palatal orthodontic miniscrew insertion using a CAD-CAM surgical guide: description of a technique. Int J Oral Maxillofac Surg. 2018 Sep;47(9):1195-1198. doi: 10.1016/j.ijom.2018.03.018. Epub 2018 Apr 11. PMID: 29653870.
83. Bae MJ, Kim JY, Park JT, Cha JY, Kim HJ, Yu HS, Hwang CJ. Accuracy of miniscrew surgical guides assessed from cone-beam computed tomography and digital models. Am J Orthod Dentofacial Orthop. 2013 Jun;143(6):893-901. doi: 10.1016/j.ajodo.2013.02.018. PMID: 23726340.
84. Qiu L, Haruyama N, Suzuki S, et al. Accuracy of orthodontic miniscrew implantation guided by stereolithographic surgical stent based on cone-beam CT-derived 3D images. Angle Orthod. Mar 2012;82(2):284-93. doi:10.2319/033111-231.1
85. Becker K, Unland J, Wilmes B, Tarraf NE, Drescher D. Is there an ideal insertion angle and position for orthodontic mini-implants in the anterior palate? A CBCT study in humans. Am J Orthod Dentofacial Orthop. 2019 Sep;156(3):345-354. doi: 10.1016/j.ajodo.2018.09.019. PMID: 31474264.
86. Lo Giudice A, Quinzi V, Ronsivalle V, Martina S, Bennici O, Isola G. Description of a Digital Work-Flow for CBCT-Guided Construction of Micro-Implant Supported Maxillary Skeletal Expander. Materials (Basel). 2020 Apr 12;13(8):1815. doi: 10.3390/ma13081815. PMID: 32290597; PMCID: PMC7215674.
87. Wilmes B, Vasudavan S, Drescher D. CAD-CAM-fabricated mini-implant insertion guides for the delivery of a distalization appliance in a single appointment. Am J Orthod Dentofacial Orthop. Jul 2019;156(1):148-156. doi:10.1016/j.ajodo.2018.12.017
88. Lee NK, Baek SH. Effects of the diameter and shape of orthodontic mini-implants on microdamage to the cortical bone. Am J Orthod Dentofacial Orthop. 2010 Jul;138(1):8.e1-8; discussion 8-9. doi: 10.1016/j.ajodo.2010.02.019. Erratum in: Am J Orthod Dentofacial Orthop. 2011 Jul;140(1):4. PMID: 20620822.
89. Copello FM, Brunetto DP, Elias CN, et al. Miniscrew-assisted rapid palatal expansion (MARPE): how to achieve greater stability. In vitro study. Dental Press J Orthod. 2021;26(1):e211967. doi:10.1590/2177-6709.26.1.e211967.oar
90. Poorsattar-Bejeh Mir A. Monocortical versus bicortical hard palate anchorage with the same total available cortical thickness: a finite element study. J Investig Clin Dent. 2017 Aug;8(3). doi: 10.1111/jicd.12218. Epub 2016 May 8. PMID: 27157504.
91. Choi JY, Choi JH, Kim NK, et al. Analysis of errors in medical rapid prototyping models. Int J Oral Maxillofac Surg. Feb 2002;31(1):23-32. doi:10.1054/ijom.2000.0135
92. Dietrich CA, Ender A, Baumgartner S, Mehl A. A validation study of reconstructed rapid prototyping models produced by two technologies. Angle Orthod. 2017 Sep;87(5):782-787. doi: 10.2319/01091-727.1. Epub 2017 May 1. PMID: 28459285; PMCID: PMC8357202.
93. Hazeveld A, Huddleston Slater JJ, Ren Y. Accuracy and reproducibility of dental replica models reconstructed by different rapid prototyping techniques. Am J Orthod Dentofacial Orthop. Jan 2014;145(1):108-15. doi:10.1016/j.ajodo.2013.05.011
94. Wan Hassan WN, Yusoff Y, Mardi NA. Comparison of reconstructed rapid prototyping models produced by 3-dimensional printing and conventional stone models with different degrees of crowding. Am J Orthod Dentofacial Orthop. Jan 2017;151(1):209-218. doi:10.1016/j.ajodo.2016.08.019
95. Chen YJ, Chang HH, Huang CY, Hung HC, Lai EH, Yao CC. A retrospective analysis of the failure rate of three different orthodontic skeletal anchorage systems. Clin Oral Implants Res. 2007 Dec;18(6):768-75. doi: 10.1111/j.1600-0501.2007.01405.x. Epub 2007 Sep 14. PMID: 17868386.
96. Lee DW, Park JH, Bay RC, Choi SK, Chae JM. Cortical bone thickness and bone density effects on miniscrew success rates: A systematic review and meta-analysis. Orthod Craniofac Res. 2021 Mar;24 Suppl 1:92-102. doi: 10.1111/ocr.12453. Epub 2020 Dec 16. PMID: 33277824.
97. Melo AC, Andrighetto AR, Hirt SD, Bongiolo AL, Silva SU, Silva MA. Risk factors associated with the failure of miniscrews - A ten-year cross sectional study. Braz Oral Res. Oct 24 2016;30(1):e124. doi:10.1590/1807-3107BOR-2016.vol30.0124
98. Crismani AG, Bertl MH, Celar AG, Bantleon HP, Burstone CJ. Miniscrews in orthodontic treatment: review and analysis of published clinical trials. Am J Orthod Dentofacial Orthop. 2010 Jan;137(1):108-13. doi: 10.1016/j.ajodo.2008.01.027. PMID: 20122438.
99. Stoetzer M, Wagner ME, Wenzel D, Lindhorst D, Gellrich NC, von See C. Nonradiological method for 3-dimensional implant position assessment using an intraoral scan: new method for postoperative implant control. Implant Dent. Oct 2014;23(5):612-6. doi:10.1097/id.0000000000000118
100. Jing Z, Wu Y, Jiang W, et al. Factors affecting the clinical success rate of miniscrew implants for orthodontic treatment. Int J Oral Maxillofac Implants. Jul-Aug 2016;31(4):835-41. doi:10.11607/jomi.4197
101. Yi J, Ge M, Li M, et al. Comparison of the success rate between self-drilling and self-tapping miniscrews: a systematic review and meta-analysis. Eur J Orthod. Jun 1 2017;39(3):287-293. doi:10.1093/ejo/cjw036
102. Chang CH, Lin JS, Roberts WE. Failure rates for stainless steel versus titanium alloy infrazygomatic crest bone screws: A single-center, randomized double-blind clinical trial. Angle Orthod. Jan 2019;89(1):40-46. doi:10.2319/012518-70.1

103. Karagkiolidou A, Ludwig B, Pazera P, Gkantidis N, Pandis N, Katsaros C. Survival of palatal miniscrews used for orthodontic appliance anchorage: a retrospective cohort study. Am J Orthod Dentofacial Orthop. Jun 2013;143(6):767-72. doi:10.1016/j.ajodo.2013.01.018
104. Arqub SA, Gandhi V, Mehta S, Palo L, Upadhyay M, Yadav S. Survival estimates and risk factors for failure of palatal and buccal mini-implants. Angle Orthod. Nov 1 2021;91(6):756-763. doi:10.2319/090720-777.1
105. Morea C, Hayek JE, Oleskovicz C, Dominguez GC, Chilvarquer I. Precise insertion of orthodontic miniscrews with a stereolithographic surgical guide based on cone beam computed tomography data: a pilot study. Int J Oral Maxillofac Implants. Jul-Aug 2011;26(4):860-5.
106. Suzuki EY, Suzuki B. Accuracy of miniscrew implant placement with a 3-dimensional surgical guide. J Oral Maxillofac Surg. Jun 2008;66(6):1245-52. doi:10.1016/j.joms.2007.08.047
107. Miyazawa K, Kawaguchi M, Tabuchi M, Goto S. Accurate pre-surgical determination for self-drilling miniscrew implant placement using surgical guides and cone-beam computed tomography. Eur J Orthod. Dec 2010;32(6):735-40. doi:10.1093/ejo/cjq012
108. De Gabriele O, Dallatana G, Riva R, Vasudavan S, Wilmes B. The easy driver for placement of palatal mini-implants and a maxillary expander in a single appointment. J Clin Orthod. Nov 2017;51(11):728-737.
109. Buschang PH, Carrillo R, Ozenbaugh B, Rossouw PE. 2008 survey of AAO members on miniscrew usage. J Clin Orthod. Sep 2008;42(9):513-8.
110. Bock NC, Ruf S. Skeletal anchorage for everybody? a questionnaire study on frequency of use and clinical indications in daily practice. J Orofac Orthop. Mar 2015;76(2):113-24, 126-8. doi:10.1007/s00056-014-0275-z
111. Meeran NA, Venkatesh KG, Jaseema Parveen MF. Current trends in miniscrew utilization among Indian orthodontists. J Orthod Sci. Apr 2012;1(2):46-50. doi:10.4103/2278-0203.99762
112. Kyung HM, Park HS, Bae SM, Sung JH, Kim IB. Development of orthodontic micro-implants for intraoral anchorage. J Clin Orthod. Jun 2003;37(6):321-8; quiz 314.
113. Bernhart T, Vollgruber A, Gahleitner A, Dörtbudak O, Haas R. Alternative to the median region of the palate for placement of an orthodontic implant. Clin Oral Implants Res. 2000 Dec;11(6):595-601. doi: 10.1034/j.1600-0501.2000.011006595.x. PMID: 11168253.
114. Garn SM, McCreery LD. Variability of postnatal ossification timing and evidence for a "dosage" effect. Am J Phys Anthropol. Jan 1970;32(1):139-44. doi:10.1002/ajpa.1330320116
115. Usui T, Uematsu S, Kanegae H, Morimoto T, Kurihara S. Change in maximum occlusal force in association with maxillofacial growth. Orthod Craniofac Res. Nov 2007;10(4):226-34. doi:10.1111/j.1601-6343.2007.00405.x
116. Pancherz H. Temporal and masseter muscle activity in children and adults with normal occlusion. An electromyographic investigation. Acta Odontol Scand. 1980;38(6):343-8. doi:10.3109/00016358009033603
117. Raadsheer MC, Kiliaridis S, Van Eijden TM, Van Ginkel FC, Prahl-Andersen B. Masseter muscle thickness in growing individuals and its relation to facial morphology. Arch Oral Biol. Apr 1996;41(4):323-32. doi:10.1016/0003-9969(95)00136-0
118. Braun S, Hnat WP, Freudenthaler JW, Marcotte MR, Hönigle K, Johnson BE. A study of maximum bite force during growth and development. Angle Orthod. 1996;66(4):261-4. doi:10.1043/0003-3219(1996)066<0261:Asombf>2.3.Co;2
119. Han S, Bayome M, Lee J, Lee YJ, Song HH, Kook YA. Evaluation of palatal bone density in adults and adolescents for application of skeletal anchorage devices. Angle Orthod. Jul 2012;82(4):625-31. doi:10.2319/071311-445.1
120. Johnston FE, Hufham HP, Jr., Moreschi AF, Terry GP. SKELETAL MATURATION AND CEPHALOFACIAL DEVELOPMENT. Angle Orthod. Jan 1965;35:1-11. doi:10.1043/0003-3219(1965)035<0001:Smacd>2.0.Co;2
121. Hägg U, Taranger J. Maturation indicators and the pubertal growth spurt. Am J Orthod. Oct 1982;82(4):299-309. doi:10.1016/0002-9416(82)90464-x
122. Fishman LS. Chronological versus skeletal age, an evaluation of craniofacial growth. Angle Orthod. Jul 1979;49(3):181-9. doi:10.1043/0003-3219(1979)049<0181:Cvsaae>2.0.Co;2
123. Perinetti G, Sbardella V, Contardo L. Diagnostic reliability of the third finger middle phalanx maturation (MPM) method in the identification of the mandibular growth peak. Eur J Orthod. Apr 1 2017;39(2):194-201. doi:10.1093/ejo/cjw059
124. Perinetti G, Contardo L. Reliability of Growth Indicators and Efficiency of Functional Treatment for Skeletal Class II Malocclusion: Current Evidence and Controversies. Biomed Res Int. 2017;2017:1367691. doi:10.1155/2017/1367691
125. Schwartz-Dabney CL, Dechow PC. Variations in cortical material properties throughout the human dentate mandible. Am J Phys Anthropol. Mar 2003;120(3):252-77. doi:10.1002/ajpa.10121
126. Deguchi T, Nasu M, Murakami K, Yabuuchi T, Kamioka H, Takano-Yamamoto T. Quantitative evaluation of cortical bone thickness with computed tomographic scanning for orthodontic implants. Am J Orthod Dentofacial Orthop. Jun 2006;129(6):721.e7-12. doi:10.1016/j.ajodo.2006.02.026
127. Samrit V, Kharbanda OP, Duggal R, Seith A, Malhotra V. Bone density and miniscrew stability in orthodontic patients. Aust Orthod J. Nov 2012;28(2):204-12.
128. Migliorati M, Benedicenti S, Signori A, et al. Miniscrew design and bone characteristics: an experimental study of primary stability. Am J Orthod Dentofacial Orthop. Aug 2012;142(2):228-34. doi:10.1016/j.ajodo.2012.03.029
129. Shah AH, Behrents RG, Kim KB, Kyung HM, Buschang PH. Effects of screw and host factors on insertion torque and pullout strength. Angle Orthod. Jul 2012;82(4):603-10. doi:10.2319/070111-427.1
130. Chang CJ, Lin WC, Chen MY, Chang HC. Evaluation of total bone and cortical bone thickness of the palate for temporary anchorage device insertion. J Dent Sci. Mar 2021;16(2):636-642. doi:10.1016/j.jds.2020.09.016

131. Arisan V, Karabuda ZC, Avsever H, Özdemir T. Conventional multi-slice computed tomography (CT) and cone-beam CT (CBCT) for computer-assisted implant placement. Part I: relationship of radiographic gray density and implant stability. Clin Implant Dent Relat Res. Dec 2013;15(6):893-906. doi:10.1111/j.1708-8208.2011.00436.x
132. Song YY, Cha JY, Hwang CJ. Mechanical characteristics of various orthodontic mini-screws in relation to artificial cortical bone thickness. Angle Orthod. Nov 2007;77(6):979-85. doi:10.2319/090606-363.1
133. Pithon MM, Nojima MG, Nojima LI. Primary stability of orthodontic mini-implants inserted into maxilla and mandible of swine. Oral Surg Oral Med Oral Pathol Oral Radiol. Jun 2012;113(6):748-54. doi:10.1016/j.tripleo.2011.06.021
134. Motoyoshi M, Yoshida T, Ono A, Shimizu N. Effect of cortical bone thickness and implant placement torque on stability of orthodontic mini-implants. Int J Oral Maxillofac Implants. Sep-Oct 2007;22(5):779-84.
135. Marquezan M, Souza MM, Araújo MT, Nojima LI, Nojima Mda C. Is miniscrew primary stability influenced by bone density? Braz Oral Res. Sep-Oct 2011;25(5):427-32. doi:10.1590/s1806-83242011000500009
136. Wilmes B, Rademacher C, Olthoff G, Drescher D. Parameters Affecting Primary Stability of Orthodontic Mini-implants. Journal of Orofacial Orthopedics / Fortschritte der Kieferorthopädie. 2006/05/01 2006;67(3):162-174. doi:10.1007/s00056-006-0611-z
137. Ichinohe M, Motoyoshi M, Inaba M, et al. Risk factors for failure of orthodontic mini-screws placed in the median palate. J Oral Sci. Mar 28 2019;61(1):13-18. doi:10.2334/josnusd.17-0377
138. Weaver CM, Gordon CM, Janz KF, et al. The National Osteoporosis Foundation's position statement on peak bone mass development and lifestyle factors: a systematic review and implementation recommendations. Osteoporos Int. Apr 2016;27(4):1281-1386. doi:10.1007/s00198-015-3440-3
139. Bailey DA, McKay HA, Mirwald RL, Crocker PR, Faulkner RA. A six-year longitudinal study of the relationship of physical activity to bone mineral accrual in growing children: the university of Saskatchewan bone mineral accrual study. J Bone Miner Res. Oct 1999;14(10):1672-9. doi:10.1359/jbmr.1999.14.10.1672